fractal and fractional

MDPI

Article

Unraveling the Dynamics of Singular Stochastic Solitons in Stochastic Fractional Kuramoto–Sivashinsky Equation

M. Mossa Al-Sawalha [1], Humaira Yasmin [2,*], Rasool Shah [3,*], Abdul Hamid Ganie [4] and Khaled Moaddy [5]

[1] Department of Mathematics, College of Science, University of Ha'il, Ha'il 2440, Saudi Arabia; m.alswalha@uoh.edu.sa
[2] Department of Basic Sciences, Preparatory Year Deanship, King Faisal University, Al-Ahsa 31982, Saudi Arabia
[3] Department of Computer Science and Mathematics, Lebanese American University, Beirut P.O. Box 13-5053, Lebanon
[4] Basic Science Department, College of Science and Theoretical Studies, Saudi Electronic University, Riyadh 11673, Saudi Arabia; a.ganie@seu.edu.sa
[5] Department of Mathematics, College of Science and Humanities, Shaqra University, Shaqra 11691, Saudi Arabia; moaddy@yahoo.com
* Correspondence: hhassain@kfu.edu.sa (H.Y.); rasool.shah@lau.edu.lb (R.S.)

Abstract: This work investigates the complex dynamics of the stochastic fractional Kuramoto–Sivashinsky equation (SFKSE) with conformable fractional derivatives. The research begins with the creation of singular stochastic soliton solutions utilizing the modified extended direct algebraic method (mEDAM). Comprehensive contour, 3D, and 2D visual representations clearly depict the categorization of these stochastic soliton solutions as kink waves or shock waves, offering a clear description of these soliton behaviors within the context of the SFKSE framework. The paper also illustrates the flexibility of the transformation-based approach mEDAM for investigating soliton occurrence not only in SFKSE but also in a wide range of nonlinear fractional partial differential equations (FPDEs). Furthermore, the analysis considers the effect of noise, specifically Brownian motion, on soliton solutions and wave dynamics, revealing the significant influence of randomness on the propagation, generation, and stability of soliton in complex stochastic systems and advancing our understanding of extreme behaviors in scientific and engineering domains.

Keywords: FPDEs; stochastic fractional Kuramoto–Sivashinsky equation; conformable fractional derivative; solitons; singular solutions; shocks; kinks

Citation: Al-Sawalha, M.M. ; Yasmin, H.; Shah, R.; Ganie, A.H.; Moaddy, K. Unraveling the Dynamics of Singular Stochastic Solitons in Stochastic Fractional Kuramoto–Sivashinsky Equation. *Fractal Fract.* **2023**, *7*, 753. https://doi.org/10.3390/fractalfract7100753

Academic Editors: Vassili Kolokoltsov and Mingshu Peng

Received: 21 September 2023
Revised: 9 October 2023
Accepted: 10 October 2023
Published: 12 October 2023

1. Introduction

Stochastic fractional differential equations (SFDEs) are a powerful mathematical framework with numerous applications in science and engineering [1–3]. They combine stochastic processes, which address unpredictability, with fractional calculus, which includes memory and non-local effects, allowing them to simulate complicated events that classical differential equations cannot. SFDEs are useful in finance for asset price modeling and risk assessment and in physics, biology, geophysics, and environmental science for understanding various natural phenomena. They are also useful in control theory, signal processing, and image analysis, providing novel solutions to difficult system and data analysis issues [4–8].

Solitons , also called solitary waves, are observed in nonlinear systems in fields as diverse as physics, optics, and other disciplines [9–11]. These incredible waves are self-sustaining waves that maintain their form and speed as they travel. They appear as robust entities in various physical circumstances, providing vital insights into wave dynamics. Solitons have piqued the curiosity of mathematicians and academics, prompting them to investigate soliton dynamics in both nonlinear FPDEs. As a result of their efforts, several analytical methods have emerged, including the tan-function method [12], exp-function method [13], sub-equation method [14], Kudryashov method [15], (G′/G)-expansion approach [16], Sardar sub-equation method [17], Khater method [18], sin-Gordon method [19], and mEDAM [20–22].

The primary goal of this investigation is to investigate and analyze the characteristics of solitons in the SFKSE. This nonlinear model is introduced as [23,24]:

$$du + [pD_x^\beta(D_x^\beta u) + uD_x^\beta u + rD_x^\beta(D_x^\beta(D_x^\beta(D_x^\beta u)))]dt = \rho u dW, \quad (1)$$

where $u \equiv u(x,t)$ denotes a real stochastic function, $D_x^\beta(\cdot)$ denotes conformable fractional derivative's operator, r and p are nonzero real constants, $W = W(t)$ denotes Brownian motion and is completely dependent on t, and ρ denotes noise intensity. The SFKSE, with parameters $\rho = 0$ and $\beta = 1$, is a versatile Kuramoto–Sivashinsky Equation (KSE) that can be used to illustrate long waves at the interface of two viscous fluids, unstable drift waves in plasmas, and Benard convection in a one-dimensional elongated box. It also helps regulate surface roughness in sputtering-grown thin solid films, generate amorphous films, and comprehend step dynamics in epitaxy.

Many researchers have successfully solved the KSE and SFKSE using various methodologies such as modified polynomial expansion method [25], the ansatz method [26], the tanh method and its modification [27], perturbation method [28], tanh-coth method [29], homotopy analysis method [30], Painlevé expansion methods [31], and many others [32] investigated accurate solutions. In this research, we provide the mEDAM [33] as a novel way to study soliton dynamics within the SFKSE. We propose using an appropriate complex transformation to turn the SFKSE into a set of nonlinear ordinary differential equations (NODEs). These NODEs are then turned into a system of nonlinear equations by assuming a series-based solution. Using the Maple tool to solve the resultant system, we construct a wide range of stochastic soliton solutions for the SFKSE. This fresh technique adds to the expanding amount of innovative ideas proposed by experts in this discipline [34–36].

The researchers discovered that singular solitons in the context of the SFKSE typically appear as kink waves or shock waves. This classification derives from the equation's delicate interaction of fractional derivatives, stochastic (random) effects, and nonlinear dynamics. Kink waves reflect localized energy concentrations and quick changes in the spatial pattern of the solution. In contrast, shock waves represent fast gradient shifts impacted by the equation's complexity. Brownian motion, or noise, introduced into the SFKSE provides unpredictability into the model, altering soliton solutions and wave dynamics. Brownian motion can cause system fluctuations, possibly affecting solitons' generation, propagation, and stability, making them more unpredictable and changeable in complex stochastic systems. This research illuminates the significant influence of noise on the behavior of solitons and wave dynamics within the SFKSE framework, providing insights into extreme occurrences in scientific and practical applications [37–39].

The rest of the study is organized as follows: Section 2 introduces the Brownian motion, conformable fractal derivative definitions, and methodology of mEDAM. Section 3 focuses on calculating the wave equation for SFKSE, while Section 4 employs the mEDAM to calculate stochastic soliton solutions for SFKSE. Section 5 contains a series of graphs that show the effect of multiplicative noise on SFKSE's soliton solutions. Finally, in the final part, we summarize our findings and offer conclusions.

2. Methodology and Resources

2.1. Brownian Motion

The stochastic process $W(t)_{t \geq 0}$ is called a Brownian motion if it satisfies the following conditions:

- $W(0) = 0$;
- $W(t)$ is continuous function;
- $W(t) - W(s)$ is independent for $s < t$;

- $W(t) - W(s)$ has a Gaussian distribution with mean 0 and variance $t - s$.

2.2. Conformable Fractional Derivative

In Equation (1), the fractional derivatives used correspond to conformable fractional derivatives. The operator that expresses these derivatives of order δ is defined in [40] as follows:

$$D_{\Omega}^{\beta}u(\Omega) = \lim_{\gamma \to 0} \frac{u(\gamma\Omega^{1-\beta} + \Omega) - u(\Omega)}{\gamma}, \quad \beta \in (0, 1]. \tag{2}$$

The following features of this derivative are used in this investigation:

$$D_{\Omega}^{\beta}\Omega^{n} = n\Omega^{n-\beta}, \tag{3}$$

$$D_{\Omega}^{\beta}(n_1\eta(\Omega) \pm n_2\gamma(\Omega)) = n_1 D_{\Omega}^{\beta}(\eta(\Omega)) \pm n_2 D_{\Omega}^{\beta}(\gamma(\Omega)), \tag{4}$$

$$D_{\Omega}^{\beta}\chi[\xi(\Omega)] = \chi'_{\xi}(\xi(\Omega))D_{\Omega}^{\beta}\xi(\Omega), \tag{5}$$

where $\eta(\Omega)$, $\gamma(\Omega)$, $\chi(\Omega)$, and $\xi(\Omega)$ represent functions that exhibit differentiability, whereas n, n_1, and n_2 signify constants.

2.3. The Working Mechanism of mEDAM

This section outlines EDAM's operational procedures. Take into account the general FPDE listed below [20–22]:

$$M(y, \partial_t^{\alpha}y, \partial_{r_1}^{\beta}y, \partial_{r_2}^{\gamma}y, y\partial_{r_1}^{\beta}y, \dots) = 0, \;\; 0 < \alpha, \beta, \gamma \leq 1, \tag{6}$$

where $y = y(t, r_1, r_2, r_3, \dots, r_i)$.

Following these steps allows us to solve Problem (6):

1. First, $y(t, r_1, r_2, r_3, \dots, r_i) = Y(\Omega)$, $\Omega = \Omega(t, r_1, r_2, r_3, \dots, r_i)$, (Ω can be written in many ways) is executed to turn (6) into a NODE of the form:

$$T(Y, Y', Y'Y, \dots) = 0, \tag{7}$$

   where Y in (7) has derivatives with respect to Ω. Equation (7) may occasionally be integrated once or more to obtain the integration's constant.
2. Then, we assume the following series form solution for (7):

$$Y(\Omega) = \sum_{m=-j}^{j} S_m(\chi(\Omega))^m, \tag{8}$$

   where $S_m(m = -j, \dots, 0, \dots, j)$ are unknown constants to be found later, and $\chi(\varphi)$ is the general solution of the subsequent ODE.

$$\chi'(\Omega) = ln(\kappa)(c(\chi(\Omega))^2 + b\chi(\Omega) + a), \tag{9}$$

   where $\kappa \neq 0, 1$ and a, b and c are invariables.
3. The positive integer j present in (8) is called balance number, which is obtained by taking the homogeneous balance between the highest order derivative and the biggest nonlinear term in (7).
4. Following that, we insert (8) into (7) or into the equation created by integrating (7), and we then compile all of the terms of $\chi(\Omega)$ that are in the same order and produce an expression in $\chi(\Omega)$. A system of algebraic equations in $S_m(m = -j, \dots, 0 \dots, j)$ and other parameters is produced by equating all the coefficients of the expression to zero using the concept of comparison of coefficients.
5. To solve this set of algebraic equations, we use Maple-13 software.

6. The soliton solutions to (6) are then explored by determining the unidentified coefficients and additional parameters and placing them in (8) together with the $\chi(\Omega)$ (general solution of (9)). The families of soliton solutions shown below may be produced using this generic solution of (9).

Family. 1 : When $\nu < 0 \quad c \neq 0$,

$$\chi_1(\Omega) = -\frac{b}{2c} + \frac{\sqrt{-\nu}\tan_\kappa\left(\frac{1}{2}\sqrt{-\nu}\Omega\right)}{2c},$$

$$\chi_2(\Omega) = -\frac{b}{2c} - \frac{\sqrt{-\nu}\cot_\kappa\left(\frac{1}{2}\sqrt{-\nu}\Omega\right)}{2c},$$

$$\chi_3(\Omega) = -\frac{b}{2c} + \frac{\sqrt{-\nu}\left(\tan_\kappa\left(\sqrt{-\nu}\Omega\right) \pm \left(\sqrt{q_1 q_2}\sec_\kappa\left(\sqrt{-\nu}\Omega\right)\right)\right)}{2c},$$

$$\chi_4(\Omega) = -\frac{b}{2c} - \frac{\sqrt{-\nu}\left(\cot_\kappa\left(\sqrt{-\nu}\Omega\right) \pm \left(\sqrt{q_1 q_2}\csc_\kappa\left(\sqrt{-\nu}\Omega\right)\right)\right)}{2c},$$

and

$$\chi_5(\Omega) = -\frac{b}{2c} + \frac{\sqrt{-\nu}\left(\tan_\kappa\left(\frac{1}{4}\sqrt{-\nu}\Omega\right) - \cot_\kappa\left(\frac{1}{4}\sqrt{-\nu}\Omega\right)\right)}{4c}.$$

Family. 2: When $\nu > 0 \quad c \neq 0$,

$$\chi_6(\Omega) = -\frac{b}{2c} - \frac{\sqrt{\nu}\tanh_\kappa\left(\frac{1}{2}\sqrt{\nu}\Omega\right)}{2c},$$

$$\chi_7(\Omega) = -\frac{b}{2c} - \frac{\sqrt{\nu}\coth_\kappa\left(\frac{1}{2}\sqrt{\nu}\Omega\right)}{2c},$$

$$\chi_8(\Omega) = -\frac{b}{2c} - \frac{\sqrt{\nu}\left(\tanh_\kappa\left(\sqrt{\nu}\Omega\right) \pm \left(\sqrt{q_1 q_2}sech_\kappa\left(\sqrt{\nu}\Omega\right)\right)\right)}{2c},$$

$$\chi_9(\Omega) = -\frac{b}{2c} - \frac{\sqrt{\nu}\left(\coth_\kappa\left(\sqrt{\nu}\Omega\right) \pm \left(\sqrt{q_1 q_2}csch_\kappa\left(\sqrt{\nu}\Omega\right)\right)\right)}{2c},$$

and

$$\chi_{10}(\Omega) = -\frac{b}{2c} - \frac{\sqrt{\nu}\left(\tanh_\kappa\left(\frac{1}{4}\sqrt{\nu}\Omega\right) - \coth_\kappa\left(\frac{1}{4}\sqrt{\nu}\Omega\right)\right)}{4c}.$$

Family. 3: When $ac > 0$ and $b = 0$,

$$\chi_{11}(\Omega) = \sqrt{\frac{a}{c}}\tan_\kappa\left(\sqrt{ac}\Omega\right),$$

$$\chi_{12}(\Omega) = -\sqrt{\frac{a}{c}}\cot_\kappa\left(\sqrt{ac}\Omega\right),$$

$$\chi_{13}(\Omega) = \sqrt{\frac{a}{c}}\left(\tan_\kappa\left(2\sqrt{ac}\Omega\right) \pm \left(\sqrt{q_1 q_2}\sec_\kappa\left(2\sqrt{ac}\Omega\right)\right)\right),$$

$$\chi_{14}(\Omega) = -\sqrt{\frac{a}{c}}\left(\cot_\kappa\left(2\sqrt{AC}\Omega\right) \pm \left(\sqrt{q_1 q_2}\csc_\kappa\left(2\sqrt{ac}\Omega\right)\right)\right),$$

and

$$\chi_{15}(\Omega) = \frac{1}{2}\sqrt{\frac{a}{c}}\left(\tan_\kappa\left(\frac{1}{2}\sqrt{ac}\Omega\right) - \cot_\kappa\left(\frac{1}{2}\sqrt{ac}\Omega\right)\right).$$

Family. 4: When $ac > 0$ and $b = 0$,

$$\chi_{16}(\Omega) = -\sqrt{-\frac{a}{c}}\tanh_\kappa\left(\sqrt{-ac}\Omega\right),$$

$$\chi_{17}(\Omega) = -\sqrt{-\frac{a}{c}}\coth_\kappa\left(\sqrt{-ac}\Omega\right),$$

$$\chi_{18}(\Omega) = -\sqrt{-\frac{a}{c}}\left(\tanh_\kappa\left(2\sqrt{-ac}\Omega\right) \pm \left(i\sqrt{q_1q_2}sech_A\left(2\sqrt{-ac}\Omega\right)\right)\right),$$

$$\chi_{19}(\Omega) = -\sqrt{-\frac{a}{c}}\left(\coth_\kappa\left(2\sqrt{-ac}\Omega\right) \pm \left(\sqrt{q_1q_2}csch_\kappa\left(2\sqrt{-ac}\Omega\right)\right)\right),$$

and

$$\chi_{20}(\Omega) = -\frac{1}{2}\sqrt{-\frac{a}{c}}\left(\tanh_\kappa\left(\frac{1}{2}\sqrt{-ac}\Omega\right) + \coth_\kappa\left(\frac{1}{2}\sqrt{-ac}\Omega\right)\right).$$

Family. 5: When $c = a$ and $b = 0$,

$$\chi_{21}(\Omega) = \tan_\kappa(a\Omega),$$

$$\chi_{22}(\Omega) = -\cot_\kappa(a\Omega),$$

$$\chi_{23}(\Omega) = \tan_\kappa(2A\Omega) \pm (\sqrt{q_1q_2}\sec_\kappa(2a\Omega)),$$

$$\chi_{24}(\Omega) = -\cot_\kappa(2a\Omega) \pm (\sqrt{q_1q_2}\csc_\kappa(2a\Omega)),$$

and

$$\chi_{25}(\Omega) = \frac{1}{2}\tan_\kappa\left(\frac{1}{2}a\Omega\right) - \frac{1}{2}\cot_\kappa\left(\frac{1}{2}a\Omega\right).$$

Family. 6: When $c = -a$ and $b = 0$,

$$\chi_{26}(\Omega) = -\tanh_\kappa(a\Omega),$$

$$\chi_{27}(\Omega) = -\coth_\kappa(a\Omega),$$

$$\chi_{28}(\Omega) = -\tanh_\kappa(2a\Omega) \pm (i\sqrt{q_1q_2}sech_\kappa(2a\Omega)),$$

$$\chi_{29}(\Omega) = -\coth_\kappa(2a\Omega) \pm (\sqrt{q_1q_2}csch_\kappa(2a\Omega)),$$

and

$$\chi_{30}(\Omega) = -\frac{1}{2}\tanh_\kappa\left(\frac{1}{2}a\Omega\right) - \frac{1}{2}\coth_\kappa\left(\frac{1}{2}a\Omega\right).$$

Family. 7: When $\nu = 0$,

$$\chi_{31}(\Omega) = -2\,\frac{a(b\Omega\, ln\kappa + 2)}{b^2\Omega\, ln\kappa}.$$

Family. 8: When $b = \nu$, $a = m\omega(m \neq 0)$ and $c = 0$,

$$\chi_{32}(\Omega) = \kappa^{\nu\,\Omega} - m.$$

Family. 9: When $b = c = 0$,

$$\chi_{33}(\Omega) = a\Omega\, ln\kappa.$$

Family. 10: When $b = a = 0$,

$$\chi_{34}(\Omega) = -\frac{1}{c\Omega\, ln\kappa}.$$

Family. 11: When $a = 0$, $b \neq 0$ and $c \neq 0$,

$$\chi_{35}(\Omega) = -\frac{q_1 b}{c(\cosh_\kappa(b\Omega) - \sinh_\kappa(b\Omega) + q_1)},$$

and

$$\chi_{36}(\Omega) = -\frac{b(\cosh_\kappa(b\Omega) + \sinh_\kappa(b\Omega))}{c(\cosh_\kappa(b\Omega) + \sinh_\kappa(b\Omega) + q_2)},$$

Family. 12: When $b = \omega$, $c = m\omega(m \neq 0)$ and $a = 0$,

$$\chi_{37}(\Omega) = \frac{q_1\kappa^{\nu\Omega}}{q_1 - mq_2\kappa^{\nu\Omega}}.$$

where $q_1, q_2 > 0$ and are referred to as deformation parameters and $\nu = b^2 - 4ac$. The generalized hyperbolic and trigonometric functions present in our solutions are expressed as below:

$$\sin_\kappa(\Omega) = \frac{q_1\kappa^{i\Omega} - q_2\kappa^{-i\Omega}}{2i}, \quad \cos_\kappa(\Omega) = \frac{q_1\kappa^{-i\Omega} + q_2\kappa^{i\Omega}}{2},$$
$$\sec_\kappa(\Omega) = \frac{1}{\cos_\kappa(\Omega)}, \quad \csc_\kappa(\Omega) = \frac{1}{\sin_\kappa(\Omega)},$$
$$\cot_\kappa(\Omega) = \frac{\cos_\kappa(\Omega)}{\sin_\kappa(\Omega)}, \quad \tan_\kappa(\Omega) = \frac{\sin_\kappa(\Omega)}{\cos_\kappa(\Omega)}.$$

Similarly,

$$\sinh_\kappa(\Omega) = \frac{q_1\kappa^{\Omega} - q_2\kappa^{-\Omega}}{2}, \quad \cosh_\kappa(\Omega) = \frac{q_1\kappa^{-\Omega} + q_2\kappa^{\Omega}}{2},$$
$$sech_\kappa(\Omega) = \frac{1}{\cosh_\kappa(\Omega)}, \quad csch_\kappa(\Omega) = \frac{1}{\sinh_\kappa(\Omega)},$$
$$\coth_\kappa(\Omega) = \frac{\cosh_\kappa(\Omega)}{\sinh_\kappa(\Omega)}, \quad \tanh_\kappa(\Omega) = \frac{\sinh_\kappa(\Omega)}{\cosh_\kappa(\Omega)}.$$

3. Wave Equation for SFKSE

To obtain the wave equation of SFSKSE (1), we utilize the following wave transformation:

$$u(x,t) = U(\Omega)e^{(\rho W(t) - \frac{\rho^2 t}{2})}, \quad \Omega = \mu t + \frac{\lambda x^\beta}{\beta}, \tag{10}$$

where U is the deterministic function. Differentiating (10) with regard to t and x, we obtain

$$\begin{aligned} du &= (\mu U' - \frac{\rho^2 t}{2} + \frac{\rho^2 t}{2})e^{(\rho W(t) - \frac{\rho^2 t}{2})}dt + \rho U e^{(\rho W(t) - \frac{\rho^2 t}{2})}dW \\ D_x^\beta u &= \lambda U' e^{(\rho W(t) - \frac{\rho^2 t}{2})}, \quad D_x^\beta(D_x^\beta u) = \lambda^2 U'' e^{(\rho W(t) - \frac{\rho^2 t}{2})} \\ D_x^\beta(D_x^\beta(D_x^\beta u)) &= \lambda^3 U''' e^{(\rho W(t) - \frac{\rho^2 t}{2})}, \quad D_x^\beta(D_x^\beta(D_x^\beta(D_x^\beta u))) = \lambda^4 U^{(iv)} e^{(\rho W(t) - \frac{\rho^2 t}{2})}, \end{aligned} \tag{11}$$

where $\frac{\rho^2 t}{2}$ is the Itô correction term. Inserting (10) into (1) and using (11), we have

$$\frac{\mu}{\lambda}U' + UU'e^{(\rho W(t) - \frac{\rho^2 t}{2})} + p\lambda U'' + r\lambda^3 U'''' = 0. \tag{12}$$

Taking expectation on both sides, we have

$$\frac{\mu}{\lambda}U' + UU'e^{-\frac{\rho^2 t}{2}}\mathbb{E}(e^{\rho W(t)}) + p\lambda U'' + r\lambda^3 U'''' = 0, \tag{13}$$

where U is the deterministic function. We note that $\mathbb{E}(e^{\rho W(t)} = e^{\frac{\rho^2 t}{2}})$, where $W(t)$ is normal standard distribution and ρ is a real constant. Now, (13) has the form

$$\frac{\mu}{\lambda}U' + UU' + p\lambda U'' + r\lambda^3 U'''' = 0. \tag{14}$$

Integrating (14) and putting the constant of integration equal zero, we obtain

$$\frac{\mu}{\lambda}U + \frac{U^2}{2} + p\lambda U' + r\lambda^3 U''' = 0, \tag{15}$$

4. Stochastic Soliton Solutions

In this section, we aim to construct stochastic soliton solutions for SFKSE presented in (1). For this we homogeneously balance the highest order derivative $r\lambda^3 U'''$ and the nonlinear term $\frac{U^2}{2}$ which implies $j + 3 = 2j$ i.e., $j = 3$. By substituting $j = 1$ in (8), we obtain the series form solution for (15) as follows:

$$W(\eta) = \sum_{m=0}^{3} S_m(\chi(\Omega))^m = S_0 + S_1(\chi(\Omega))^1 + S_2(\chi(\Omega))^2 + S_3(\chi(\Omega))^3. \tag{16}$$

We generate an expression in $\chi(\Omega)$ by placing (16) in (15) and collecting every term with the same powers of $\chi(\Omega)$. A system of nonlinear algebraic equations is formed by equating all coefficients to zero. Using Maple to solve the system yields the following two sets of solutions:

Case. 1

$$\begin{aligned} &S_0 = 30\,\frac{\left(-6\,bca + b^3 + \sqrt{\nu^3}\right)(\ln(\kappa))^3\lambda^3}{r}, S_1 = -360\,\frac{\lambda^3(\ln(\kappa))^3 ac^2}{r}, S_2 = -180\,\frac{\lambda^3(\ln(\kappa))^3 bc^2}{r}, \\ &S_3 = -120\,\frac{\lambda^3(\ln(\kappa))^3 c^3}{r}, p = -19\,\frac{\lambda^2(\ln(\kappa))^2\nu}{r}, \lambda = \lambda, \mu = -30\,\frac{\lambda^4(\ln(\kappa))^3\sqrt{\nu^3}}{r} \end{aligned} \tag{17}$$

Case. 2

$$\begin{aligned} &S_0 = \frac{30}{11}\,\frac{\left(-b^3 - 18\,bca + \sqrt{\nu^3}\right)(\ln(\kappa))^3\lambda^3}{r}, S_1 = -\frac{360}{11}\,\frac{\lambda^3(\ln(\kappa))^3 c\left(3\,ca + 2\,b^2\right)}{r}, \lambda = \lambda, \\ &S_2 = \frac{-180\,\lambda^3(\ln(\kappa))^3 bc^2}{r}, S_3 = \frac{-120\,\lambda^3(\ln(\kappa))^3 c^3}{r}, p = \frac{19}{11}\,\frac{\lambda^2(\ln(\kappa))^2\nu}{r}, \mu = -\frac{30}{11}\,\frac{\lambda^4(\ln(\kappa))^3\sqrt{\nu^3}}{r} \end{aligned} \tag{18}$$

Considering Case 1 and using (10) and (16) and the corresponding solution of (9), we obtain the following families of singular stochastic soliton solutions for (1):

Family. 1.1: When $\nu < 0 \quad c \neq 0$,

$$u_{1,1}(x,t) = e^{(\rho W(t) - \frac{\rho^2 t}{2})}(-15\,\frac{\lambda^3(\ln(\kappa))^3\left(-2\,\sqrt{\nu^3} - 3\,\nu\,\sqrt{-\nu}\tan_\kappa\left(\frac{1}{2}\,\sqrt{-\nu}\Omega\right) + (-\nu)^{3/2}\left(\tan_\kappa\left(\frac{1}{2}\sqrt{-\nu}\Omega\right)\right)^3\right)}{r}), \tag{19}$$

$$u_{1,2}(x,t) = e^{(\rho W(t) - \frac{\rho^2 t}{2})}(15\,\frac{\lambda^3(\ln(\kappa))^3\left(2\,\sqrt{\nu^3} - 3\,\nu\,\sqrt{-\nu}\cot_\kappa\left(\frac{1}{2}\sqrt{-\nu}\Omega\right) + (-\nu)^{3/2}\left(\cot_\kappa\left(\frac{1}{2}\sqrt{-\nu}\Omega\right)\right)^3\right)}{r}), \tag{20}$$

$$u_{1,3}(x,t) = e^{(\rho W(t) - \frac{\rho^2 t}{2})}(30\,\frac{\left(-6\,bca + b^3 + \sqrt{\nu^3}\right)(\ln(\kappa))^3\lambda^3}{r}$$
$$\frac{-360\,\lambda^3(\ln(\kappa))^3ac^2\left(-\frac{1}{2}\frac{b}{c} + \frac{1}{2}\frac{\sqrt{-\nu}\left(\tan_\kappa\left(\sqrt{-\nu}\Omega\right)+\sqrt{q_1q_2}\sec_\kappa\left(\sqrt{-\nu}\Omega\right)\right)}{c}\right)}{r}$$
$$\frac{-180\,\lambda^3(\ln(\kappa))^3bc^2\left(-\frac{1}{2}\frac{b}{c} + \frac{1}{2}\frac{\sqrt{-\nu}\left(\tan_\kappa\left(\sqrt{-\nu}\Omega\right)+\sqrt{q_1q_2}\sec_\kappa\left(\sqrt{-\nu}\Omega\right)\right)}{c}\right)^2}{r} \tag{21}$$
$$\frac{-120\,\lambda^3(\ln(\kappa))^3c^3\left(-\frac{1}{2}\frac{b}{c} + \frac{1}{2}\frac{\sqrt{-\nu}\left(\tan_\kappa\left(\sqrt{-\nu}\Omega\right)+\sqrt{q_1q_2}\sec_\kappa\left(\sqrt{-\nu}\Omega\right)\right)}{c}\right)^3}{r}),$$

$$u_{1,4}(x,t) = e^{(\rho W(t) - \frac{\rho^2 t}{2})}(30\,\frac{\left(-6\,bca + b^3 + \sqrt{\nu^3}\right)(\ln(\kappa))^3\lambda^3}{r}$$
$$\frac{-360\,\lambda^3(\ln(\kappa))^3ac^2\left(-\frac{1}{2}\frac{b}{c} - \frac{1}{2}\frac{\sqrt{-\nu}\left(\cot_\kappa\left(\sqrt{-\nu}\Omega\right)+\sqrt{q_1q_2}\csc_\kappa\left(\sqrt{-\nu}\Omega\right)\right)}{c}\right)}{r}$$
$$\frac{-180\,\lambda^3(\ln(\kappa))^3bc^2\left(-\frac{1}{2}\frac{b}{c} - \frac{1}{2}\frac{\sqrt{-\nu}\left(\cot_\kappa\left(\sqrt{-\nu}\Omega\right)+\sqrt{q_1q_2}\csc_\kappa\left(\sqrt{-\nu}\Omega\right)\right)}{c}\right)^2}{r} \tag{22}$$
$$\frac{-120\,\lambda^3(\ln(\kappa))^3c^3\left(-\frac{1}{2}\frac{b}{c} - \frac{1}{2}\frac{\sqrt{-\nu}\left(\cot_\kappa\left(\sqrt{-\nu}\Omega\right)+\sqrt{q_1q_2}\csc_\kappa\left(\sqrt{-\nu}\Omega\right)\right)}{c}\right)^3}{r}),$$

and

$$u_{1,5}(x,t) = e^{(\rho W(t) - \frac{\rho^2 t}{2})}(30\,\frac{\left(-6\,bca + b^3 + \sqrt{\nu^3}\right)(\ln(\kappa))^3\lambda^3}{r}$$
$$\frac{-360\,\lambda^3(\ln(\kappa))^3ac^2\left(-\frac{1}{2}\frac{b}{c} + \frac{1}{4}\frac{\sqrt{-\nu}\left(\tan_\kappa\left(\frac{1}{4}\sqrt{-\nu}\Omega\right)-\cot_\kappa\left(\frac{1}{4}\sqrt{-\nu}\Omega\right)\right)}{c}\right)}{r}$$
$$\frac{-180\,\lambda^3(\ln(\kappa))^3bc^2\left(-\frac{1}{2}\frac{b}{c} + \frac{1}{4}\frac{\sqrt{-\nu}\left(\tan_\kappa\left(\frac{1}{4}\sqrt{-\nu}\Omega\right)-\cot_\kappa\left(\frac{1}{4}\sqrt{-\nu}\Omega\right)\right)}{c}\right)^2}{r} \tag{23}$$
$$\frac{-120\,\lambda^3(\ln(\kappa))^3c^3\left(-\frac{1}{2}\frac{b}{c} + \frac{1}{4}\frac{\sqrt{-\nu}\left(\tan_\kappa\left(\frac{1}{4}\sqrt{-\nu}\Omega\right)-\cot_\kappa\left(\frac{1}{4}\sqrt{-\nu}\Omega\right)\right)}{c}\right)^3}{r}),$$

Family. 1.2: When $\nu > 0 \quad c \neq 0$,

$$u_{1,6}(x,t) = e^{(\rho W(t) - \frac{\rho^2 t}{2})}(15\,\frac{\lambda^3(\ln(\kappa))^3\left(2\sqrt{\nu^3} - 3\,\nu^{3/2}\tanh_\kappa\left(\frac{1}{2}\sqrt{\nu}\Omega\right) + \nu^{3/2}\left(\tanh_\kappa\left(\frac{1}{2}\sqrt{\nu}\Omega\right)\right)^3\right)}{r}), \tag{24}$$

$$u_{1,7}(x,t) = e^{(\rho W(t) - \frac{\rho^2 t}{2})}(15\,\frac{\lambda^3(\ln(\kappa))^3\left(2\sqrt{\nu^3} - 3\,\nu^{3/2}\coth_\kappa\left(\frac{1}{2}\sqrt{\nu}\Omega\right) + \nu^{3/2}\left(\coth_\kappa\left(\frac{1}{2}\sqrt{\nu}\Omega\right)\right)^3\right)}{r}), \tag{25}$$

$$u_{1,8}(x,t) = e^{(\rho W(t) - \frac{\rho^2 t}{2})}(30\,\frac{\left(-6\,bca + b^3 + \sqrt{\nu^3}\right)(\ln(\kappa))^3\lambda^3}{r}$$
$$\frac{-360\,\lambda^3(\ln(\kappa))^3 ac^2\left(-\frac{1}{2}\frac{b}{c} - \frac{1}{2}\frac{\sqrt{\nu}\left(\tanh_\kappa\left(\sqrt{\nu}\Omega\right)+\sqrt{-q_1q_2}sech_\kappa\left(\sqrt{\nu}\Omega\right)\right)}{c}\right)}{r}$$
$$\frac{-180\,\lambda^3(\ln(\kappa))^3 bc^2\left(-\frac{1}{2}\frac{b}{c} - \frac{1}{2}\frac{\sqrt{\nu}\left(\tanh_\kappa\left(\sqrt{\nu}\Omega\right)+\sqrt{-q_1q_2}sech_\kappa\left(\sqrt{\nu}\Omega\right)\right)}{c}\right)^2}{r} \tag{26}$$
$$\frac{-120\,\lambda^3(\ln(\kappa))^3 c^3\left(-\frac{1}{2}\frac{b}{c} - \frac{1}{2}\frac{\sqrt{\nu}\left(\tanh_\kappa\left(\sqrt{\nu}\Omega\right)+\sqrt{-q_1q_2}sech_\kappa\left(\sqrt{\nu}\Omega\right)\right)}{c}\right)^3}{r}),$$

$$u_{1,9}(x,t) = e^{(\rho W(t) - \frac{\rho^2 t}{2})}(30\,\frac{\left(-6\,bca + b^3 + \sqrt{\nu^3}\right)(\ln(\kappa))^3\lambda^3}{r}$$
$$\frac{-360\,\lambda^3(\ln(\kappa))^3 ac^2\left(-\frac{1}{2}\frac{b}{c} - \frac{1}{2}\frac{\sqrt{\nu}\left(\coth_\kappa\left(\sqrt{\nu}\Omega\right)+\sqrt{q_1q_2}csch_\kappa\left(\sqrt{\nu}\Omega\right)\right)}{c}\right)}{r}$$
$$\frac{-180\,\lambda^3(\ln(\kappa))^3 bc^2\left(-\frac{1}{2}\frac{b}{c} - \frac{1}{2}\frac{\sqrt{\nu}\left(\coth_\kappa\left(\sqrt{\nu}\Omega\right)+\sqrt{q_1q_2}csch_\kappa\left(\sqrt{\nu}\Omega\right)\right)}{c}\right)^2}{r} \tag{27}$$
$$\frac{-120\,\lambda^3(\ln(\kappa))^3 c^3\left(-\frac{1}{2}\frac{b}{c} - \frac{1}{2}\frac{\sqrt{\nu}\left(\coth_\kappa\left(\sqrt{\nu}\Omega\right)+\sqrt{q_1q_2}csch_\kappa\left(\sqrt{\nu}\Omega\right)\right)}{c}\right)^3}{r}),$$

and

$$u_{1,10}(x,t) = e^{(\rho W(t) - \frac{\rho^2 t}{2})}(30\,\frac{\left(-6\,bca + b^3 + \sqrt{\nu^3}\right)(\ln(\kappa))^3\lambda^3}{r}$$
$$\frac{-360\,\lambda^3(\ln(\kappa))^3 ac^2\left(-\frac{1}{2}\frac{b}{c} - \frac{1}{4}\frac{\sqrt{\nu}\left(\tanh_\kappa\left(\frac{1}{4}\sqrt{\nu}\Omega\right)-\coth_\kappa\left(\frac{1}{4}\sqrt{\nu}\Omega\right)\right)}{c}\right)}{r}$$
$$\frac{-180\,\lambda^3(\ln(\kappa))^3 bc^2\left(-\frac{1}{2}\frac{b}{c} - \frac{1}{4}\frac{\sqrt{\nu}\left(\tanh_\kappa\left(\frac{1}{4}\sqrt{\nu}\Omega\right)-\coth_\kappa\left(\frac{1}{4}\sqrt{\nu}\Omega\right)\right)}{c}\right)^2}{r} \tag{28}$$
$$\frac{-120\,\lambda^3(\ln(\kappa))^3 c^3\left(-\frac{1}{2}\frac{b}{c} - \frac{1}{4}\frac{\sqrt{\nu}\left(\tanh_\kappa\left(\frac{1}{4}\sqrt{\nu}\Omega\right)-\coth_\kappa\left(\frac{1}{4}\sqrt{\nu}\Omega\right)\right)}{c}\right)^3}{r}),$$

Family. 1.3 : When $ac > 0$ and $b = 0$,

$$u_{1,11}(x,t) = e^{(\rho W(t) - \frac{\rho^2 t}{2})}(\frac{120\,(\ln(\kappa))^3\lambda^3\left(2\sqrt{-a^3c^3} - 3\,ac^2\sqrt{\frac{a}{c}}\tan_\kappa\left(\sqrt{ac}\Omega\right) - c^2a\sqrt{\frac{a}{c}}\left(\tan_\kappa\left(\sqrt{ac}\Omega\right)\right)^3\right)}{r}), \tag{29}$$

$$u_{1,12}(x,t) = e^{(\rho W(t) - \frac{\rho^2 t}{2})}(\frac{120\,(\ln(\kappa))^3\lambda^3\left(2\sqrt{-a^3c^3} + 3\,ac^2\sqrt{\frac{a}{c}}\cot_\kappa\left(\sqrt{ac}\Omega\right) + c^2a\sqrt{\frac{a}{c}}\left(\cot_\kappa\left(\sqrt{ac}\Omega\right)\right)^3\right)}{r}), \tag{30}$$

$$u_{1,13}(x,t) = e^{(\rho W(t)-\frac{\rho^2 t}{2})}\Big(-\frac{360\,\lambda^3(\ln(\kappa))^3 ac^2\sqrt{\frac{a}{c}}\left(\tan_\kappa\left(2\sqrt{ac}\Omega\right)+\sqrt{q_1q_2}\sec_\kappa\left(2\sqrt{ac}\Omega\right)\right)}{r} - \frac{120\,\lambda^3(\ln(\kappa))^3 c^3\left(\frac{a}{c}\right)^{3/2}\left(\tan_\kappa\left(2\sqrt{ac}\Omega\right)+\sqrt{q_1q_2}\sec_\kappa\left(2\sqrt{ac}\Omega\right)\right)^3}{r} + 240\,\frac{\sqrt{-a^3c^3}(\ln(\kappa))^3\lambda^3}{r}\Big), \tag{31}$$

$$u_{1,14}(x,t) = e^{(\rho W(t)-\frac{\rho^2 t}{2})}\Big(\frac{360\,\lambda^3(\ln(\kappa))^3 ac^2\sqrt{\frac{a}{c}}\left(\cot_\kappa\left(2\sqrt{ac}\Omega\right)+\sqrt{q_1q_2}\csc_\kappa\left(2\sqrt{ac}\Omega\right)\right)}{r} + \frac{120\,\lambda^3(\ln(\kappa))^3 c^3\left(\frac{a}{c}\right)^{3/2}\left(\cot_\kappa\left(2\sqrt{ac}\Omega\right)+\sqrt{q_1q_2}\csc_\kappa\left(2\sqrt{ac}\Omega\right)\right)^3}{r} + 240\,\frac{\sqrt{-a^3c^3}(\ln(\kappa))^3\lambda^3}{r}\Big), \tag{32}$$

and

$$u_{1,15}(x,t) = e^{(\rho W(t)-\frac{\rho^2 t}{2})}\Big(-\frac{180\,\lambda^3(\ln(\kappa))^3 ac^2\sqrt{\frac{a}{c}}\left(\tan_\kappa\left(\frac{1}{2}\sqrt{ac}\Omega\right)-\cot_\kappa\left(\frac{1}{2}\sqrt{ac}\Omega\right)\right)}{r} - \frac{15\,\lambda^3(\ln(\kappa))^3 c^3\left(\frac{a}{c}\right)^{3/2}\left(\tan_\kappa\left(\frac{1}{2}\sqrt{ac}\Omega\right)-\cot_\kappa\left(\frac{1}{2}\sqrt{ac}\Omega\right)\right)^3}{r} + 240\,\frac{\sqrt{-a^3c^3}(\ln(\kappa))^3\lambda^3}{r}\Big), \tag{33}$$

Family. 1.4: When $ac < 0$ and $b = 0$,

$$u_{1,16}(x,t) = e^{(\rho W(t)-\frac{\rho^2 t}{2})}\Big(\frac{120\sqrt{-(ac)^3}(\ln(\kappa))^3\lambda^3\left(2+3\tanh_\kappa\left(\sqrt{-ac}\Omega\right)-\left(\tanh_\kappa\left(\sqrt{-ac}\Omega\right)\right)^3\right)}{r}\Big), \tag{34}$$

$$u_{1,17}(x,t) = e^{(\rho W(t)-\frac{\rho^2 t}{2})}\Big(\frac{120\sqrt{-(ac)^3}(\ln(\kappa))^3\lambda^3\left(2+3\coth_\kappa\left(\sqrt{-ac}\Omega\right)-\left(\coth_\kappa\left(\sqrt{-ac}\Omega\right)\right)^3\right)}{r}\Big), \tag{35}$$

$$u_{1,18}(x,t) = e^{(\rho W(t)-\frac{\rho^2 t}{2})}\Big(\frac{360\,\lambda^3(\ln(\kappa))^3 ac^2\sqrt{-\frac{a}{c}}\left(\tanh_\kappa\left(2\sqrt{-ac}\Omega\right)+\sqrt{-q_1q_2}sech_\kappa\left(2\sqrt{-ac}\Omega\right)\right)}{r} + \frac{120\,\lambda^3(\ln(\kappa))^3 c^3\left(-\frac{a}{c}\right)^{3/2}\left(\tanh_\kappa\left(2\sqrt{-ac}\Omega\right)+\sqrt{-q_1q_2}sech_\kappa\left(2\sqrt{-ac}\Omega\right)\right)^3}{r} + 240\,\frac{\sqrt{-a^3c^3}(\ln(\kappa))^3\lambda^3}{r}\Big), \tag{36}$$

$$u_{1,19}(x,t) = e^{(\rho W(t)-\frac{\rho^2 t}{2})}\Big(\frac{360\,\lambda^3(\ln(\kappa))^3 ac^2\sqrt{-\frac{a}{c}}\left(\coth_\kappa\left(2\sqrt{-ac}\Omega\right)+\sqrt{q_1q_2}csch_\kappa\left(2\sqrt{-ac}\Omega\right)\right)}{r} + \frac{120\,\lambda^3(\ln(\kappa))^3 c^3\left(-\frac{a}{c}\right)^{3/2}\left(\coth_\kappa\left(2\sqrt{-ac}\Omega\right)+\sqrt{q_1q_2}csch_\kappa\left(2\sqrt{-ac}\Omega\right)\right)^3}{r} + 240\,\frac{\sqrt{-a^3c^3}(\ln(\kappa))^3\lambda^3}{r}\Big), \tag{37}$$

and

$$u_{1,20}(x,t) = e^{(\rho W(t)-\frac{\rho^2 t}{2})}\Big(\frac{180\,\lambda^3(\ln(\kappa))^3 ac^2\sqrt{-\frac{a}{c}}\left(\tanh_\kappa\left(\frac{1}{2}\sqrt{-ac}\Omega\right)+\coth_\kappa\left(\frac{1}{2}\sqrt{-ac}\Omega\right)\right)}{r} + \frac{15\,\lambda^3(\ln(\kappa))^3 c^3\left(-\frac{a}{c}\right)^{3/2}\left(\tanh_\kappa\left(\frac{1}{2}\sqrt{-ac}\Omega\right)+\coth_\kappa\left(\frac{1}{2}\sqrt{-ac}\Omega\right)\right)^3}{r} + 240\,\frac{\sqrt{-a^3c^3}(\ln(\kappa))^3\lambda^3}{r}\Big), \tag{38}$$

Family. 1.5: When $c = a$ and $b = 0$,

$$u_{1,21}(x,t) = e^{(\rho W(t) - \frac{\rho^2 t}{2})}(120\,\frac{(\ln(\kappa))^3 \lambda^3 \left(2\sqrt{-a^6} - 3\,a^3 \tan_\kappa(a\Omega) - a^3 (\tan_\kappa(a\Omega))^3\right)}{r}), \tag{39}$$

$$u_{1,22}(x,t) = e^{(\rho W(t) - \frac{\rho^2 t}{2})}(120\,\frac{(\ln(\kappa))^3 \lambda^3 \left(2\sqrt{-a^6} + 3\,a^3 \cot_\kappa(a\Omega) + a^3 (\cot_\kappa(a\Omega))^3\right)}{r}), \tag{40}$$

$$\begin{aligned} u_{1,23}(x,t) = e^{(\rho W(t) - \frac{\rho^2 t}{2})}(-360\,&\frac{\lambda^3 (\ln(\kappa))^3 a^3 \left(\tan_\kappa(2\,a\Omega) + \sqrt{q_1 q_2}\sec_\kappa(2\,a\Omega)\right)}{r} \\ - 120\,\frac{\lambda^3 (\ln(\kappa))^3 a^3 \left(\tan_\kappa(2\,a\Omega) + \sqrt{q_1 q_2}\sec_\kappa(2\,a\Omega)\right)^3}{r} &+ 240\,\frac{\sqrt{-a^6}(\ln(\kappa))^3 \lambda^3}{r}), \end{aligned} \tag{41}$$

$$\begin{aligned} u_{1,24}(x,t) = e^{(\rho W(t) - \frac{\rho^2 t}{2})}(-360\,&\frac{\lambda^3 (\ln(\kappa))^3 a^3 \left(-\cot_\kappa(2\,a\Omega) - \sqrt{q_1 q_2}\csc_\kappa(2\,a\Omega)\right)}{r} \\ - 120\,\frac{\lambda^3 (\ln(\kappa))^3 a^3 \left(-\cot_\kappa(2\,a\Omega) - \sqrt{q_1 q_2}\csc_\kappa(2\,a\Omega)\right)^3}{r} &+ 240\,\frac{\sqrt{-a^6}(\ln(\kappa))^3 \lambda^3}{r}), \end{aligned} \tag{42}$$

and

$$\begin{aligned} u_{1,25}(x,t) = e^{(\rho W(t) - \frac{\rho^2 t}{2})}(-360\,&\frac{\lambda^3 (\ln(\kappa))^3 a^3 \left(\frac{1}{2}\tan_\kappa(1/2\,a\Omega) - \frac{1}{2}\cot_\kappa\left(\frac{1}{2}a\Omega\right)\right)}{r} \\ - 120\,\frac{\lambda^3 (\ln(\kappa))^3 a^3 \left(\frac{1}{2}\tan_\kappa\left(\frac{1}{2}a\Omega\right) - \frac{1}{2}\cot_\kappa\left(\frac{1}{2}a\Omega\right)\right)^3}{r} &+ 240\,\frac{\sqrt{-a^6}(\ln(\kappa))^3 \lambda^3}{r}), \end{aligned} \tag{43}$$

Family. 1.6: When $c = -a$ and $b = 0$,

$$u_{1,26}(x,t) = e^{(\rho W(t) - \frac{\rho^2 t}{2})}(120\,\frac{a^3 (\ln(\kappa))^3 \lambda^3 \left(2\,csgn\left(a^3\right) + 3\,\tanh_\kappa(a\Omega) - (\tanh_\kappa(a\Omega))^3\right)}{r}), \tag{44}$$

$$u_{1,27}(x,t) = e^{(\rho W(t) - \frac{\rho^2 t}{2})}(120\,\frac{a^3 (\ln(\kappa))^3 \lambda^3 \left(2\,csgn\left(a^3\right) + 3\,\coth_\kappa(a\Omega) - (\coth_\kappa(a\Omega))^3\right)}{r}), \tag{45}$$

$$\begin{aligned} u_{1,28}(x,t) = e^{(\rho W(t) - \frac{\rho^2 t}{2})}(-360\,&\frac{a^3 (\ln(\kappa))^3 \lambda^3 (-\tanh_\kappa(2\,a\Omega) - \sqrt{-q_1 q_2}sech_\kappa(2\,a\Omega))}{r} \\ + 120\,\frac{a^3 (\ln(\kappa))^3 \lambda^3 (-\tanh_\kappa(2\,a\Omega) - \sqrt{-q_1 q_2}sech_\kappa(2\,a\Omega))^3}{r} &+ 240\,\frac{a^3 (\ln(\kappa))^3 \lambda^3}{r}), \end{aligned} \tag{46}$$

$$\begin{aligned} u_{1,29}(x,t) = e^{(\rho W(t) - \frac{\rho^2 t}{2})}(-360\,&\frac{a^3 (\ln(\kappa))^3 \lambda^3 \left(-\coth_\kappa(2\,a\Omega) - \sqrt{q_1 q_2}csch_\kappa(2\,a\Omega)\right)}{r} \\ + 120\,\frac{a^3 (\ln(\kappa))^3 \lambda^3 \left(-\coth_\kappa(2\,a\Omega) - \sqrt{q_1 q_2}csch_\kappa(2\,a\Omega)\right)^3}{r} &+ 240\,\frac{a^3 (\ln(\kappa))^3 \lambda^3}{r}), \end{aligned} \tag{47}$$

and

$$u_{1,30}(x,t) = e^{(\rho W(t) - \frac{\rho^2 t}{2})}(-360\,\frac{a^3(\ln(\kappa))^3\lambda^3\left(-\frac{1}{2}\tanh_\kappa\left(\frac{1}{2}a\Omega\right) - \frac{1}{2}\coth_\kappa\left(\frac{1}{2}a\Omega\right)\right)}{r}$$
$$+ 120\,\frac{a^3(\ln(\kappa))^3\lambda^3\left(-\frac{1}{2}\tanh_\kappa\left(\frac{1}{2}a\Omega\right) - \frac{1}{2}\coth_\kappa\left(\frac{1}{2}a\Omega\right)\right)^3}{r} + 240\,\frac{a^3(\ln(\kappa))^3\lambda^3}{r}), \tag{48}$$

Family. 1.7: When $\nu = 0$,

$$u_{1,31}(x,t) = e^{(\rho W(t) - \frac{\rho^2 t}{2})}(30\,\frac{\left(-6\,bca + b^3\right)(\ln(\kappa))^3\lambda^3}{r} + 720\,\frac{\lambda^3(\ln(\kappa))^2 ac^2 a(b\Omega\,\ln(\kappa) + 2)}{rb^2\Omega}$$
$$- 720\,\frac{\lambda^3\ln(\kappa)c^2(a(b\Omega\,\ln(\kappa)+2))^2}{b^3 r\Omega^2} + 960\,\frac{\lambda^3 c^3(a(b\Omega\,\ln(\kappa)+2))^3}{rb^6\Omega^3}), \tag{49}$$

Family. 1.8: When $b = a = 0$,

$$u_{1,32}(x,t) = e^{(\rho W(t) - \frac{\rho^2 t}{2})}(30\,\frac{\lambda^3\left(\sqrt{\nu^3}(\ln(\kappa))^3\Omega^3 + 4\right)}{r\Omega^3}), \tag{50}$$

Family. 1.9: When $a = 0$, $b \neq 0$ and $c \neq 0$,

$$u_{1,33}(x,t) = e^{(\rho W(t) - \frac{\rho^2 t}{2})}(30\,\frac{\left(b^3 + \sqrt{\nu^3}\right)(\ln(\kappa))^3\lambda^3}{r}$$
$$- 180\,\frac{\lambda^3(\ln(\kappa))^3 b^3 {q_1}^2}{r(\cosh_\kappa(b\Omega) - \sinh_\kappa(b\Omega) + q_1)^2} + 120\,\frac{\lambda^3(\ln(\kappa))^3 {q_1}^3 b^3}{r(\cosh_\kappa(b\Omega) - \sinh_\kappa(b\Omega) + q_1)^3}), \tag{51}$$

and

$$u_{1,34}(x,t) = e^{(\rho W(t) - \frac{\rho^2 t}{2})}(30\,\frac{\left(b^3 + \sqrt{\nu^3}\right)(\ln(\kappa))^3\lambda^3}{r}$$
$$- 180\,\frac{\lambda^3(\ln(\kappa))^3 b^3(\cosh_\kappa(b\Omega) + \sinh_\kappa(b\Omega))^2}{r(\cosh_\kappa(b\Omega) + \sinh_\kappa(b\Omega) + q_2)^2} + 120\,\frac{\lambda^3(\ln(\kappa))^3 b^3(\cosh_\kappa(b\Omega) + \sinh_\kappa(b\Omega))^3}{r(\cosh_\kappa(b\Omega) + \sinh_\kappa(b\Omega) + q_2)^3}), \tag{52}$$

Family. 1.10: When $b = \omega$, $c = m\omega(m \neq 0)$ and $a = 0$,

$$u_{1,35}(x,t) = e^{(\rho W(t) - \frac{\rho^2 t}{2})}(30\,\frac{\left(\omega^3 + \sqrt{\nu^3}\right)(\ln(\kappa))^3\lambda^3}{r}$$
$$- 180\,\frac{\lambda^3(\ln(\kappa))^3\omega^3 m^2 {q_1}^2\left(\kappa^{\omega\,\Omega}\right)^2}{r(p - mq_2\kappa^{\omega\,\Omega})^2} - 120\,\frac{\lambda^3(\ln(\kappa))^3 m^3\omega^3 {q_1}^3\left(\kappa^{\omega\,\Omega}\right)^3}{r(p - mq_2\kappa^{\omega\,\Omega})^3}), \tag{53}$$

where $\Omega = -30\,\frac{\lambda^4(\ln(\kappa))^3\sqrt{\nu^3}}{r}t + \frac{\lambda x^\beta}{\beta}$.

Considering Case 2 and using (10), (16), and the corresponding solution of (9), we obtain the following families of singular stochastic soliton solutions for (1):

Family. 2.1: When $\nu < 0 \quad c \neq 0$,

$$u_{2,1}(x,t) = e^{(\rho W(t) - \frac{\rho^2 t}{2})}(-15\,\frac{\lambda^3(\ln(\kappa))^3\left(-2\sqrt{\nu^3} - 3\,\nu\sqrt{-\nu}\tan_\kappa\left(\frac{1}{2}\sqrt{-\nu}\Omega\right) + (-\nu)^{3/2}\left(\tan_\kappa\left(\frac{1}{2}\sqrt{-\nu}\Omega\right)\right)^3\right)}{r}), \tag{54}$$

$$u_{2,2}(x,t) = e^{(\rho W(t) - \frac{\rho^2 t}{2})}\left(15\,\frac{\lambda^3 (\ln(\kappa))^3 \left(2\sqrt{\nu^3} - 3\,\nu\sqrt{-\nu}\cot_\kappa\left(\frac{1}{2}\sqrt{-\nu}\Omega\right) + (-\nu)^{3/2}\left(\cot_\kappa\left(\frac{1}{2}\sqrt{-\nu}\Omega\right)\right)^3\right)}{r}\right), \tag{55}$$

$$\begin{aligned} u_{2,3}(x,t) = e^{(\rho W(t) - \frac{\rho^2 t}{2})}\Bigg(30\,&\frac{\left(-6\,bca + b^3 + \sqrt{\nu^3}\right)(\ln(\kappa))^3 \lambda^3}{r} \\ &- \frac{360\,\lambda^3 (\ln(\kappa))^3 ac^2 \left(-\frac{1}{2}\frac{b}{c} + \frac{1}{2}\frac{\sqrt{-\nu}\left(\tan_\kappa\left(\sqrt{-\nu}\Omega\right) + \sqrt{q_1 q_2}\sec_\kappa\left(\sqrt{-\nu}\Omega\right)\right)}{c}\right)}{r} \\ &- \frac{180\,\lambda^3 (\ln(\kappa))^3 bc^2 \left(-\frac{1}{2}\frac{b}{c} + \frac{1}{2}\frac{\sqrt{-\nu}\left(\tan_\kappa\left(\sqrt{-\nu}\Omega\right) + \sqrt{q_1 q_2}\sec_\kappa\left(\sqrt{-\nu}\Omega\right)\right)}{c}\right)^2}{r} \\ &- \frac{120\,\lambda^3 (\ln(\kappa))^3 c^3 \left(-\frac{1}{2}\frac{b}{c} + \frac{1}{2}\frac{\sqrt{-\nu}\left(\tan_\kappa\left(\sqrt{-\nu}\Omega\right) + \sqrt{q_1 q_2}\sec_\kappa\left(\sqrt{-\nu}\Omega\right)\right)}{c}\right)^3}{r}\Bigg), \end{aligned} \tag{56}$$

$$\begin{aligned} u_{2,4}(x,t) = e^{(\rho W(t) - \frac{\rho^2 t}{2})}\Bigg(30\,&\frac{\left(-6\,bca + b^3 + \sqrt{\nu^3}\right)(\ln(\kappa))^3 \lambda^3}{r} \\ &- \frac{360\,\lambda^3 (\ln(\kappa))^3 ac^2 \left(-\frac{1}{2}\frac{b}{c} - \frac{1}{2}\frac{\sqrt{-\nu}\left(\cot_\kappa\left(\sqrt{-\nu}\Omega\right) + \sqrt{q_1 q_2}\csc_\kappa\left(\sqrt{-\nu}\Omega\right)\right)}{c}\right)}{r} \\ &- \frac{180\,\lambda^3 (\ln(\kappa))^3 bc^2 \left(-\frac{1}{2}\frac{b}{c} - \frac{1}{2}\frac{\sqrt{-\nu}\left(\cot_\kappa\left(\sqrt{-\nu}\Omega\right) + \sqrt{q_1 q_2}\csc_\kappa\left(\sqrt{-\nu}\Omega\right)\right)}{c}\right)^2}{r} \\ &- \frac{120\,\lambda^3 (\ln(\kappa))^3 c^3 \left(-\frac{1}{2}\frac{b}{c} - \frac{1}{2}\frac{\sqrt{-\nu}\left(\cot_\kappa\left(\sqrt{-\nu}\Omega\right) + \sqrt{q_1 q_2}\csc_\kappa\left(\sqrt{-\nu}\Omega\right)\right)}{c}\right)^3}{r}\Bigg), \end{aligned} \tag{57}$$

and

$$\begin{aligned} u_{2,5}(x,t) = e^{(\rho W(t) - \frac{\rho^2 t}{2})}\Bigg(30\,&\frac{\left(-6\,bca + b^3 + \sqrt{\nu^3}\right)(\ln(\kappa))^3 \lambda^3}{r} \\ &- \frac{360\,\lambda^3 (\ln(\kappa))^3 ac^2 \left(-\frac{1}{2}\frac{b}{c} + \frac{1}{4}\frac{\sqrt{-\nu}\left(\tan_\kappa\left(\frac{1}{4}\sqrt{-\nu}\Omega\right) - \cot_\kappa\left(\frac{1}{4}\sqrt{-\nu}\Omega\right)\right)}{c}\right)}{r} \\ &- \frac{180\,\lambda^3 (\ln(\kappa))^3 bc^2 \left(-\frac{1}{2}\frac{b}{c} + \frac{1}{4}\frac{\sqrt{-\nu}\left(\tan_\kappa\left(\frac{1}{4}\sqrt{-\nu}\Omega\right) - \cot_\kappa\left(\frac{1}{4}\sqrt{-\nu}\Omega\right)\right)}{c}\right)^2}{r} \\ &- \frac{120\,\lambda^3 (\ln(\kappa))^3 c^3 \left(-\frac{1}{2}\frac{b}{c} + \frac{1}{4}\frac{\sqrt{-\nu}\left(\tan_\kappa\left(\frac{1}{4}\sqrt{-\nu}\Omega\right) - \cot_\kappa\left(\frac{1}{4}\sqrt{-\nu}\Omega\right)\right)}{c}\right)^3}{r}\Bigg), \end{aligned} \tag{58}$$

Family. 2.2: When $\nu > 0 \quad c \neq 0$,

$$u_{2,6}(x,t) = e^{(\rho W(t) - \frac{\rho^2 t}{2})}\left(15\,\frac{\lambda^3 (\ln(\kappa))^3 \left(2\sqrt{\nu^3} - 3\,\nu^{3/2}\tanh_\kappa\left(\frac{1}{2}\sqrt{\nu}\Omega\right) + \nu^{3/2}\left(\tanh_\kappa\left(\frac{1}{2}\sqrt{\nu}\Omega\right)\right)^3\right)}{r}\right), \tag{59}$$

$$u_{2,7}(x,t)=e^{(\rho W(t)-\frac{\rho^2 t}{2})}(15\,\frac{\lambda^3(\ln(\kappa))^3\left(2\sqrt{\nu^3}-3\,\nu^{3/2}\coth_\kappa\left(\frac{1}{2}\sqrt{\nu}\Omega\right)+\nu^{3/2}\left(\coth_\kappa\left(\frac{1}{2}\sqrt{\nu}\Omega\right)\right)^3\right)}{r}), \tag{60}$$

$$\begin{aligned}u_{2,8}(x,t)=e^{(\rho W(t)-\frac{\rho^2 t}{2})}(30\,&\frac{\left(-6\,bca+b^3+\sqrt{\nu^3}\right)(\ln(\kappa))^3\lambda^3}{r}\\ &-\frac{360\,\lambda^3(\ln(\kappa))^3ac^2\left(-\frac{1}{2}\frac{b}{c}-\frac{1}{2}\frac{\sqrt{\nu}\left(\tanh_\kappa\left(\sqrt{\nu}\Omega\right)+\sqrt{-q_1q_2}sech_\kappa\left(\sqrt{\nu}\Omega\right)\right)}{c}\right)}{r}\\ &-\frac{180\,\lambda^3(\ln(\kappa))^3bc^2\left(-\frac{1}{2}\frac{b}{c}-\frac{1}{2}\frac{\sqrt{\nu}\left(\tanh_\kappa\left(\sqrt{\nu}\Omega\right)+\sqrt{-q_1q_2}sech_\kappa\left(\sqrt{\nu}\Omega\right)\right)}{c}\right)^2}{r}\\ &-\frac{120\,\lambda^3(\ln(\kappa))^3c^3\left(-\frac{1}{2}\frac{b}{c}-\frac{1}{2}\frac{\sqrt{\nu}\left(\tanh_\kappa\left(\sqrt{\nu}\Omega\right)+\sqrt{-q_1q_2}sech_\kappa\left(\sqrt{\nu}\Omega\right)\right)}{c}\right)^3}{r}),\end{aligned} \tag{61}$$

$$\begin{aligned}u_{2,9}(x,t)=e^{(\rho W(t)-\frac{\rho^2 t}{2})}(30\,&\frac{\left(-6\,bca+b^3+\sqrt{\nu^3}\right)(\ln(\kappa))^3\lambda^3}{r}\\ &-\frac{360\,\lambda^3(\ln(\kappa))^3ac^2\left(-\frac{1}{2}\frac{b}{c}-\frac{1}{2}\frac{\sqrt{\nu}\left(\coth_\kappa\left(\sqrt{\nu}\Omega\right)+\sqrt{q_1q_2}csch_\kappa\left(\sqrt{\nu}\Omega\right)\right)}{c}\right)}{r}\\ &-\frac{180\,\lambda^3(\ln(\kappa))^3bc^2\left(-\frac{1}{2}\frac{b}{c}-\frac{1}{2}\frac{\sqrt{\nu}\left(\coth_\kappa\left(\sqrt{\nu}\Omega\right)+\sqrt{q_1q_2}csch_\kappa\left(\sqrt{\nu}\Omega\right)\right)}{c}\right)^2}{r}\\ &-\frac{120\,\lambda^3(\ln(\kappa))^3c^3\left(-\frac{1}{2}\frac{b}{c}-\frac{1}{2}\frac{\sqrt{\nu}\left(\coth_\kappa\left(\sqrt{\nu}\Omega\right)+\sqrt{q_1q_2}csch_\kappa\left(\sqrt{\nu}\Omega\right)\right)}{c}\right)^3}{r}),\end{aligned} \tag{62}$$

and

$$\begin{aligned}u_{2,10}(x,t)=e^{(\rho W(t)-\frac{\rho^2 t}{2})}(30\,&\frac{\left(-6\,bca+b^3+\sqrt{\nu^3}\right)(\ln(\kappa))^3\lambda^3}{r}\\ &-\frac{360\,\lambda^3(\ln(\kappa))^3ac^2\left(-\frac{1}{2}\frac{b}{c}-\frac{1}{4}\frac{\sqrt{\nu}\left(\tanh_\kappa\left(\frac{1}{4}\sqrt{\nu}\Omega\right)-\coth_\kappa\left(\frac{1}{4}\sqrt{\nu}\Omega\right)\right)}{c}\right)}{r}\\ &-\frac{180\,\lambda^3(\ln(\kappa))^3bc^2\left(-\frac{1}{2}\frac{b}{c}-\frac{1}{4}\frac{\sqrt{\nu}\left(\tanh_\kappa\left(\frac{1}{4}\sqrt{\nu}\Omega\right)-\coth_\kappa\left(\frac{1}{4}\sqrt{\nu}\Omega\right)\right)}{c}\right)^2}{r}\\ &-\frac{120\,\lambda^3(\ln(\kappa))^3c^3\left(-\frac{1}{2}\frac{b}{c}-\frac{1}{4}\frac{\sqrt{\nu}\left(\tanh_\kappa\left(\frac{1}{4}\sqrt{\nu}\Omega\right)-\coth_\kappa\left(\frac{1}{4}\sqrt{\nu}\Omega\right)\right)}{c}\right)^3}{r}),\end{aligned} \tag{63}$$

Family. 2.3: When $ac>0$ and $b=0$,

$$u_{2,11}(x,t)=e^{(\rho W(t)-\frac{\rho^2 t}{2})}(\frac{120\,(\ln(\kappa))^3\lambda^3\left(2\sqrt{-c^3a^3}-3\,ac^2\sqrt{\frac{a}{c}}\tan_\kappa\left(\sqrt{ca}\Omega\right)-c^2a\sqrt{\frac{a}{c}}\left(\tan_\kappa\left(\sqrt{ca}\Omega\right)\right)^3\right)}{r}), \tag{64}$$

$$u_{2,12}(x,t) = e^{(\rho W(t) - \frac{\rho^2 t}{2})}\left(\frac{120\,(\ln(\kappa))^3\lambda^3\Big(2\sqrt{-c^3a^3} + 3\,ac^2\sqrt{\frac{a}{c}}\cot_\kappa\left(\sqrt{ca}\Omega\right) + c^2a\sqrt{\frac{a}{c}}\left(\cot_\kappa\left(\sqrt{ca}\Omega\right)\right)^3\Big)}{r}\right), \tag{65}$$

$$\begin{aligned} u_{2,13}(x,t) = e^{(\rho W(t) - \frac{\rho^2 t}{2})}\Big(&240\,\frac{\sqrt{-c^3a^3}(\ln(\kappa))^3\lambda^3}{r} \\ &- \frac{360\,\lambda^3(\ln(\kappa))^3ac^2\sqrt{\frac{a}{c}}\left(\tan_\kappa\left(2\sqrt{ca}\Omega\right) + \sqrt{q_1q_2}\sec_\kappa\left(2\sqrt{ca}\Omega\right)\right)}{r} \\ &- \frac{120\,\lambda^3(\ln(\kappa))^3c^3\left(\frac{a}{c}\right)^{3/2}\left(\tan_\kappa\left(2\sqrt{ca}\Omega\right) + \sqrt{q_1q_2}\sec_\kappa\left(2\sqrt{ca}\Omega\right)\right)^3}{r}\Big), \end{aligned} \tag{66}$$

$$\begin{aligned} u_{2,14}(x,t) = e^{(\rho W(t) - \frac{\rho^2 t}{2})}\Big(&240\,\frac{\sqrt{-c^3a^3}(\ln(\kappa))^3\lambda^3}{r} \\ &+ \frac{360\,\lambda^3(\ln(\kappa))^3ac^2\sqrt{\frac{a}{c}}\left(\cot_\kappa\left(2\sqrt{ca}\Omega\right) + \sqrt{q_1q_2}\csc_\kappa\left(2\sqrt{ca}\Omega\right)\right)}{r} \\ &+ \frac{120\,\lambda^3(\ln(\kappa))^3c^3\left(\frac{a}{c}\right)^{3/2}\left(\cot_\kappa\left(2\sqrt{ca}\Omega\right) + \sqrt{q_1q_2}\csc_\kappa\left(2\sqrt{ca}\Omega\right)\right)^3}{r}\Big), \end{aligned} \tag{67}$$

and

$$\begin{aligned} u_{2,15}(x,t) = e^{(\rho W(t) - \frac{\rho^2 t}{2})}\Big(&240\,\frac{\sqrt{-c^3a^3}(\ln(\kappa))^3\lambda^3}{r} \\ &- \frac{180\,\lambda^3(\ln(\kappa))^3ac^2\sqrt{\frac{a}{c}}\Big(\tan_\kappa\Big(\frac{1}{2}\sqrt{ca}\Omega\Big) - \cot_\kappa\Big(\frac{1}{2}\sqrt{ca}\Omega\Big)\Big)}{r} \\ &- \frac{15\,\lambda^3(\ln(\kappa))^3c^3\left(\frac{a}{c}\right)^{3/2}\Big(\tan_\kappa\Big(\frac{1}{2}\sqrt{ca}\Omega\Big) - \cot_\kappa\Big(\frac{1}{2}\sqrt{ca}\Omega\Big)\Big)^3}{r}\Big), \end{aligned} \tag{68}$$

Family. 2.4: When $ac < 0$ and $b = 0$,

$$u_{2,16}(x,t) = e^{(\rho W(t) - \frac{\rho^2 t}{2})}\left(\frac{120\sqrt{-(ac)^3}(\ln(\kappa))^3\lambda^3\Big(2 + 3\,\tanh_\kappa\left(\sqrt{-ca}\Omega\right) - \left(\tanh_\kappa\left(\sqrt{-ca}\Omega\right)\right)^3\Big)}{r}\right), \tag{69}$$

$$u_{2,17}(x,t) = e^{(\rho W(t) - \frac{\rho^2 t}{2})}\left(\frac{120\sqrt{-(ac)^3}(\ln(\kappa))^3\lambda^3\Big(2 + 3\,\coth_\kappa\left(\sqrt{-ca}\Omega\right) - \left(\coth_\kappa\left(\sqrt{-ca}\Omega\right)\right)^3\Big)}{r}\right), \tag{70}$$

$$\begin{aligned} u_{2,18}(x,t) = e^{(\rho W(t) - \frac{\rho^2 t}{2})}\Big(&240\,\frac{\sqrt{-c^3a^3}(\ln(\kappa))^3\lambda^3}{r} \\ &+ \frac{360\,\lambda^3(\ln(\kappa))^3ac^2\sqrt{-\frac{a}{c}}\left(\tanh_\kappa\left(2\sqrt{-ca}\Omega\right) + \sqrt{-q_1q_2}sech_\kappa\left(2\sqrt{-ca}\Omega\right)\right)}{r} \\ &+ \frac{120\,\lambda^3(\ln(\kappa))^3c^3\left(-\frac{a}{c}\right)^{3/2}\left(\tanh_\kappa\left(2\sqrt{-ca}\Omega\right) + \sqrt{-q_1q_2}sech_\kappa\left(2\sqrt{-ca}\Omega\right)\right)^3}{r}\Big), \end{aligned} \tag{71}$$

$$u_{2,19}(x,t) = e^{(\rho W(t) - \frac{\rho^2 t}{2})}(240\,\frac{\sqrt{-c^3a^3}(\ln(\kappa))^3\lambda^3}{r} + \frac{360\,\lambda^3(\ln(\kappa))^3ac^2\sqrt{-\frac{a}{c}}\left(\coth_\kappa\left(2\sqrt{-ca}\Omega\right) + \sqrt{q_1q_2}csch_\kappa\left(2\sqrt{-ca}\Omega\right)\right)}{r} + \frac{120\,\lambda^3(\ln(\kappa))^3c^3\left(-\frac{a}{c}\right)^{3/2}\left(\coth_\kappa\left(2\sqrt{-ca}\Omega\right) + \sqrt{q_1q_2}csch_\kappa\left(2\sqrt{-ca}\Omega\right)\right)^3}{r}), \tag{72}$$

and

$$u_{2,20}(x,t) = e^{(\rho W(t) - \frac{\rho^2 t}{2})}(240\,\frac{\sqrt{-c^3a^3}(\ln(\kappa))^3\lambda^3}{r} + \frac{180\,\lambda^3(\ln(\kappa))^3ac^2\sqrt{-\frac{a}{c}}\left(\tanh_\kappa\left(\frac{1}{2}\sqrt{-ca}\Omega\right) + \coth_\kappa\left(\frac{1}{2}\sqrt{-ca}\Omega\right)\right)}{r} + \frac{15\,\lambda^3(\ln(\kappa))^3c^3\left(-\frac{a}{c}\right)^{3/2}\left(\tanh_\kappa\left(\frac{1}{2}\sqrt{-ca}\Omega\right) + \coth_\kappa\left(\frac{1}{2}\sqrt{-ca}\Omega\right)\right)^3}{r}), \tag{73}$$

Family. 2.5: When $c = a$ and $b = 0$,

$$u_{2,21}(x,t) = e^{(\rho W(t) - \frac{\rho^2 t}{2})}(120\,\frac{(\ln(\kappa))^3\lambda^3\left(2\sqrt{-a^6} - 3\,a^3\tan_\kappa(a\Omega) - a^3(\tan_\kappa(a\Omega))^3\right)}{r}), \tag{74}$$

$$u_{2,22}(x,t) = e^{(\rho W(t) - \frac{\rho^2 t}{2})}(120\,\frac{(\ln(\kappa))^3\lambda^3\left(2\sqrt{-a^6} + 3\,a^3\cot_\kappa(a\Omega) + a^3(\cot_\kappa(a\Omega))^3\right)}{r}), \tag{75}$$

$$u_{2,23}(x,t) = e^{(\rho W(t) - \frac{\rho^2 t}{2})}(240\,\frac{\sqrt{-a^6}(\ln(\kappa))^3\lambda^3}{r} - 360\,\frac{\lambda^3(\ln(\kappa))^3a^3\left(\tan_\kappa(2\,a\Omega) + \sqrt{q_1q_2}\sec_\kappa(2\,a\Omega)\right)}{r} - 120\,\frac{\lambda^3(\ln(\kappa))^3a^3\left(\tan_\kappa(2\,a\Omega) + \sqrt{q_1q_2}\sec_\kappa(2\,a\Omega)\right)^3}{r}), \tag{76}$$

$$u_{2,24}(x,t) = e^{(\rho W(t) - \frac{\rho^2 t}{2})}(240\,\frac{\sqrt{-a^6}(\ln(\kappa))^3\lambda^3}{r} - 360\,\frac{\lambda^3(\ln(\kappa))^3a^3\left(-\cot_\kappa(2\,a\Omega) - \sqrt{q_1q_2}\csc_\kappa(2\,a\Omega)\right)}{r} - 120\,\frac{\lambda^3(\ln(\kappa))^3a^3\left(-\cot_\kappa(2\,a\Omega) - \sqrt{q_1q_2}\csc_\kappa(2\,a\Omega)\right)^3}{r}), \tag{77}$$

and

$$u_{2,25}(x,t) = e^{(\rho W(t) - \frac{\rho^2 t}{2})}(240\,\frac{\sqrt{-a^6}(\ln(\kappa))^3\lambda^3}{r} - 360\,\frac{\lambda^3(\ln(\kappa))^3a^3\left(\frac{1}{2}\tan_\kappa(1/2\,a\Omega) - \frac{1}{2}\cot_\kappa\left(\frac{1}{2}a\Omega\right)\right)}{r} - 120\,\frac{\lambda^3(\ln(\kappa))^3a^3\left(\frac{1}{2}\tan_\kappa\left(\frac{1}{2}a\Omega\right) - \frac{1}{2}\cot_\kappa\left(\frac{1}{2}a\Omega\right)\right)^3}{r}), \tag{78}$$

Family. 2.6: When $c = -a$ and $b = 0$,

$$u_{2,26}(x,t) = e^{(\rho W(t) - \frac{\rho^2 t}{2})}(30\,\frac{(\ln(\kappa))^3\lambda^3\left(\sqrt{\nu^3} + 12\,a^3\tanh_\kappa(a\Omega) - 4\,a^3(\tanh_\kappa(a\Omega))^3\right)}{r}), \tag{79}$$

$$u_{2,27}(x,t) = e^{(\rho W(t) - \frac{\rho^2 t}{2})}(30\,\frac{(\ln(\kappa))^3\lambda^3\left(\sqrt{\nu^3} + 12\,a^3\coth_\kappa(a\Omega) - 4\,a^3(\coth_\kappa(a\Omega))^3\right)}{r}), \tag{80}$$

$$\begin{aligned} u_{2,28}(x,t) = {} & e^{(\rho W(t) - \frac{\rho^2 t}{2})}(30\,\frac{\sqrt{\nu^3}(\ln(\kappa))^3\lambda^3}{r} - 360\,\frac{\lambda^3(\ln(\kappa))^3a^3(-\tanh_\kappa(2\,a\Omega) - \sqrt{-q_1q_2}sech_\kappa(2\,a\Omega))}{r} \\ & + 120\,\frac{\lambda^3(\ln(\kappa))^3a^3(-\tanh_\kappa(2\,a\Omega) - \sqrt{-q_1q_2}sech_\kappa(2\,a\Omega))^3}{r}), \end{aligned} \tag{81}$$

$$\begin{aligned} u_{2,29}(x,t) = {} & e^{(\rho W(t) - \frac{\rho^2 t}{2})}(240\,\frac{\sqrt{a^6}(\ln(\kappa))^3\lambda^3}{r} - 360\,\frac{\lambda^3(\ln(\kappa))^3a^3(-\coth_\kappa(2\,a\Omega) - \sqrt{q_1q_2}csch_\kappa(2\,a\Omega))}{r} \\ & + 120\,\frac{\lambda^3(\ln(\kappa))^3a^3(-\coth_\kappa(2\,a\Omega) - \sqrt{q_1q_2}csch_\kappa(2\,a\Omega))^3}{r}), \end{aligned} \tag{82}$$

and

$$\begin{aligned} u_{2,30}(x,t) = {} & e^{(\rho W(t) - \frac{\rho^2 t}{2})}(240\,\frac{\sqrt{a^6}(\ln(\kappa))^3\lambda^3}{r} - 360\,\frac{\lambda^3(\ln(\kappa))^3a^3\left(-\frac{1}{2}\tanh_\kappa\left(\frac{1}{2}a\Omega\right) - \frac{1}{2}\coth_\kappa\left(\frac{1}{2}a\Omega\right)\right)}{r} \\ & + 120\,\frac{\lambda^3(\ln(\kappa))^3a^3\left(-\frac{1}{2}\tanh_\kappa\left(\frac{1}{2}a\Omega\right) - 1/2\,\coth_\kappa\left(\frac{1}{2}a\Omega\right)\right)^3}{r}, \end{aligned} \tag{83}$$

Family. 2.7: When $\nu = 0$,

$$\begin{aligned} u_{2,31}(x,t) = {} & e^{(\rho W(t) - \frac{\rho^2 t}{2})}(30\,\frac{(-6\,bca + b^3)(\ln(\kappa))^3\lambda^3}{r} + 720\,\frac{\lambda^3(\ln(\kappa))^2ac^2a(b\Omega\,\ln(\kappa) + 2)}{rb^2\Omega} \\ & - 720\,\frac{\lambda^3\ln(\kappa)c^2(a(b\Omega\,\ln(\kappa) + 2))^2}{b^3r\Omega^2} + 960\,\frac{\lambda^3c^3(a(b\Omega\,\ln(\kappa) + 2))^3}{rb^6\Omega^3}), \end{aligned} \tag{84}$$

Family. 2.8: When $b = a = 0$,

$$u_{2,32}(x,t) = e^{(\rho W(t) - \frac{\rho^2 t}{2})}(30\,\frac{\lambda^3\left(\sqrt{\nu^3}(\ln(\kappa))^3\Omega^3 + 4\right)}{r\Omega^3}), \tag{85}$$

Family. 2.9: When $a = 0$, $b \neq 0$ and $c \neq 0$,

$$\begin{aligned} u_{2,33}(x,t) = {} & e^{(\rho W(t) - \frac{\rho^2 t}{2})}(30\,\frac{\left(b^3 + \sqrt{\nu^3}\right)(\ln(\kappa))^3\lambda^3}{r} \\ & - 180\,\frac{\lambda^3(\ln(\kappa))^3b^3{q_1}^2}{r(\cosh_\kappa(b\Omega) - \sinh_\kappa(b\Omega) + q_1)^2} + 120\,\frac{\lambda^3(\ln(\kappa))^3{q_1}^3b^3}{r(\cosh_\kappa(b\Omega) - \sinh_\kappa(b\Omega) + q_1)^3}), \end{aligned} \tag{86}$$

and

$$\begin{aligned} u_{2,34}(x,t) = {} & e^{(\rho W(t) - \frac{\rho^2 t}{2})}(30\,\frac{\left(b^3 + \sqrt{\nu^3}\right)(\ln(\kappa))^3\lambda^3}{r} \\ & - 180\,\frac{\lambda^3(\ln(\kappa))^3b^3(\cosh_\kappa(b\Omega) + \sinh_\kappa(b\Omega))^2}{r(\cosh_\kappa(b\Omega) + \sinh_\kappa(b\Omega) + q_2)^2} + 120\,\frac{\lambda^3(\ln(\kappa))^3b^3(\cosh_\kappa(b\Omega) + \sinh_\kappa(b\Omega))^3}{r(\cosh_\kappa(b\Omega) + \sinh_\kappa(b\Omega) + q_2)^3}), \end{aligned} \tag{87}$$

Family. 2.10: When $b = \lambda$, $c = n\lambda(n \neq 0)$ and $a = 0$,

$$u_{2,35}(x,t) = e^{(\rho W(t) - \frac{\rho^2 t}{2})}(30\,\frac{\left(\omega^3 + \sqrt{\nu^3}\right)(\ln(\kappa))^3\lambda^3}{r} - 180\,\frac{\lambda^3(\ln(\kappa))^3\omega^3 m^2 {q_1}^2 \left(\kappa^{\omega\,\Omega}\right)^2}{r\left(p - mq_2\kappa^{\omega\,\Omega}\right)^2} - 120\,\frac{\lambda^3(\ln(\kappa))^3 m^3\omega^3 {q_1}^3 \left(\kappa^{\omega\,\Omega}\right)^3}{r\left(p - mq_2\kappa^{\omega\,\Omega}\right)^3}), \tag{88}$$

where $\Omega = -\frac{30}{11}\frac{\lambda^4(\ln(\kappa))^3\sqrt{\nu^3}}{r}t + \frac{\lambda x^\beta}{\beta}$.

5. Discussion and Graphs

We launched a detailed examination of the SFKSE in this article, embracing conformable fractional derivatives. We have successfully generated singular stochastic soliton solutions for the SFKSE using the powerful mEDAM. These solitons have been classified into several varieties, including kink, shock, and periodic solitons, each with its own fascinating wave properties. To help in the intuitive comprehension of these solutions, we have used a variety of graphical representations, both in contour, 3D, and 2D forms, displaying their distinct wave behaviors.

The figures' visualizations clearly depict the complicated dynamics of single stochastic solitons in the SFKSE. These solitons have intriguing features and behaviors that shed light on the complicated interplay between nonlinearity and stochasticity in FPDEs. Furthermore, our research demonstrates the adaptability of the transformation-based technique, mEDAM, as a reliable and user-friendly tool for researching soliton events in a wide range of nonlinear FPDEs. This study not only increases our understanding of soliton dynamics in stochastic systems, but also highlights the potential use of mEDAM in a variety of disciplines where nonlinear FPDEs are found, opening up new possibilities for investigation and discovery.

Our study has revealed that singular solitons typically emerge as kink waves or shock waves in the region of SFKSE. The delicate interplay between the equation's fractional derivatives, stochastic effects, and nonlinear dynamics accounts for this restricted classification of solitons into these two separate categories. The unique mix of these elements creates conditions that favor the formation of kink waves, which are characterized by localized energy concentrations, or shock waves, which indicate fast gradient shifts. This solitons duality illustrates the underlying complexity and diversity of SFKSE solutions, encapsulating the main behaviors in a system where these two kinds embody the key dynamics, making them the prevalent and distinguishing expressions.

In the context of the SFKSE, a kink wave is a localized wave-like structure that signifies a quick transition or abrupt shift in the solution's spatial pattern. It happens as a result of the SFKSE's interaction of nonlinearity, diffusion, and stochastic (random) effects. The kink wave represents areas where the system's behavior varies drastically from one condition to the next. These transitions may occur due to the system's intrinsic unpredictability or as a result of intricate interactions between fractional derivatives and stochastic disturbances. The study of kink waves in SFKSE can shed light on the complicated dynamics of stochastic soliton solutions in this complex equation, shedding light on the influence of randomness on the generation, propagation, and stability of solitary wave structures.

In the context of the SFKSE, a singular shock wave is a highly localized and intense disruption in the spatial pattern that implies a quick shift in the gradient of the solution. It happens as a result of SFKSE's complicated interaction of fractional derivatives, stochastic disturbances, and nonlinear terms. Singular shock waves draw attention to the occurrence of uncommon and severe occurrences inside stochastic soliton solutions, emphasizing the system's tremendous variability and unpredictability. These waves can develop as a result of precise combinations of stochastic fluctuations and nonlinear dynamics, demonstrating the SFKSE's complex and nuanced behavior in the face of randomness. Singular shock wave analysis in SFKSE gives significant insights into the extreme occurrences and unusual phenomena that can appear in complex stochastic systems, with implications for understanding and forecasting extreme behaviors in a variety of scientific and engineering contexts.

In Figure 1, the three-dimensional representation of $u_{1,5}$ in Equation (23) is shown with the parameters' values: $a = 3, b = 1, c = 2, \lambda = 10, \kappa = e, r = 4, \beta = 1, \rho = 0$. Similarly, the two-dimensional graph is constructed using $t = 70$ and the previously specified parameter values. Overall, this profile shows a singular kink soliton. Figure 2, The three-dimensional representation of $u_{1,16}$ in Equation (34) is shown with the parameters' values: $a = -50$, $b = 0, c = 40, \lambda = 100, \kappa = e, r = 10, \beta = 0.9, \rho = 0$. Similarly, the two-dimensional graph is constructed using $t = 100$ and the previously specified parameter values. Overall, this profile shows a kink soliton. Figure 3, the three-dimensional representation of $u_{1,32}$ in Equation (50) is shown with the parameters' values: $a = 0, b = 0, c = 200, \lambda = 50$, $\kappa = 2, r = 120, \beta = 1, \rho = 1$. Similarly, the two-dimensional graph is constructed using $x = -100$ and the previously specified parameter values. Overall, this profile shows a shock soliton. Figure 4, the three-dimensional representation of $u_{2,29}$ in Equation (82) is shown with the parameters' values: $a = 70, b = 0, c = -70, \lambda = 100, \kappa = e, r = 200$, $\beta = 0.9, \rho = 0, q_1 = 100, q_2 = 90$. Similarly, the two-dimensional graph is constructed using $t = 6$ and the previously specified parameter values. Overall, this profile shows a periodic kink soliton. Figure 5, three-dimensional and contour representations of $u_{2,16}$ in Equation (69) is shown with the parameters' values: $a = -1, b = 0, c = 5, \lambda = 5, \kappa = e, r = 7$, $\beta = 0.8, \rho = 0, q_1 = 5$. Overall, this profile shows a singular shock soliton. Figure 6, the three-dimensional representation of $u_{2,35}$ in Equation (88) is shown with the parameters' values: $a = 0, b = 200, c = 800, \omega = 200, m = 4, \lambda = 160, \kappa = 3, r = 23, \rho = 0, \beta = 1$, $q_1 = 100$, $q_2 = 45$. Similarly, the two-dimensional graph is constructed using $t = 0$ and the previously specified parameter values. Overall, this profile shows a singular kink soliton.

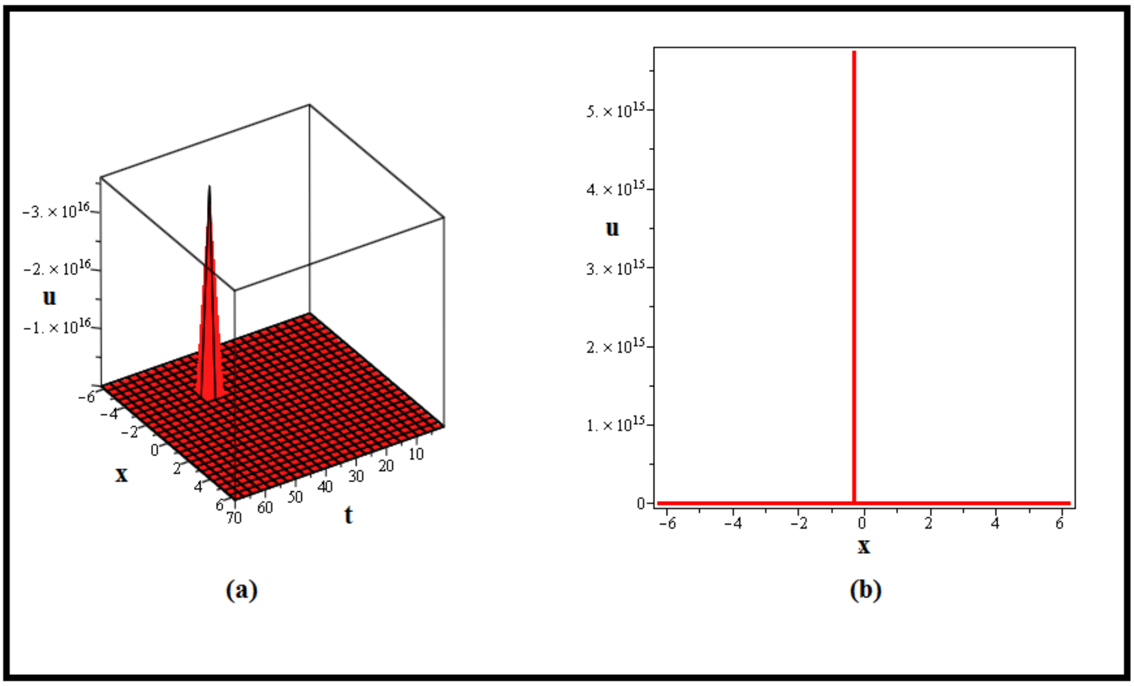

Figure 1. (**a**) The three-dimensional representation of $u_{1,5}$ in Equation (23) is shown with the parameters' values: $a = 3, b = 1, c = 2, \lambda = 10, \kappa = e, r = 4, \beta = 1, \rho = 0$. Similarly, (**b**) the two-dimensional graph is constructed using $t = 70$ and the previously specified parameter values. Overall, this profile shows a singular kink soliton.

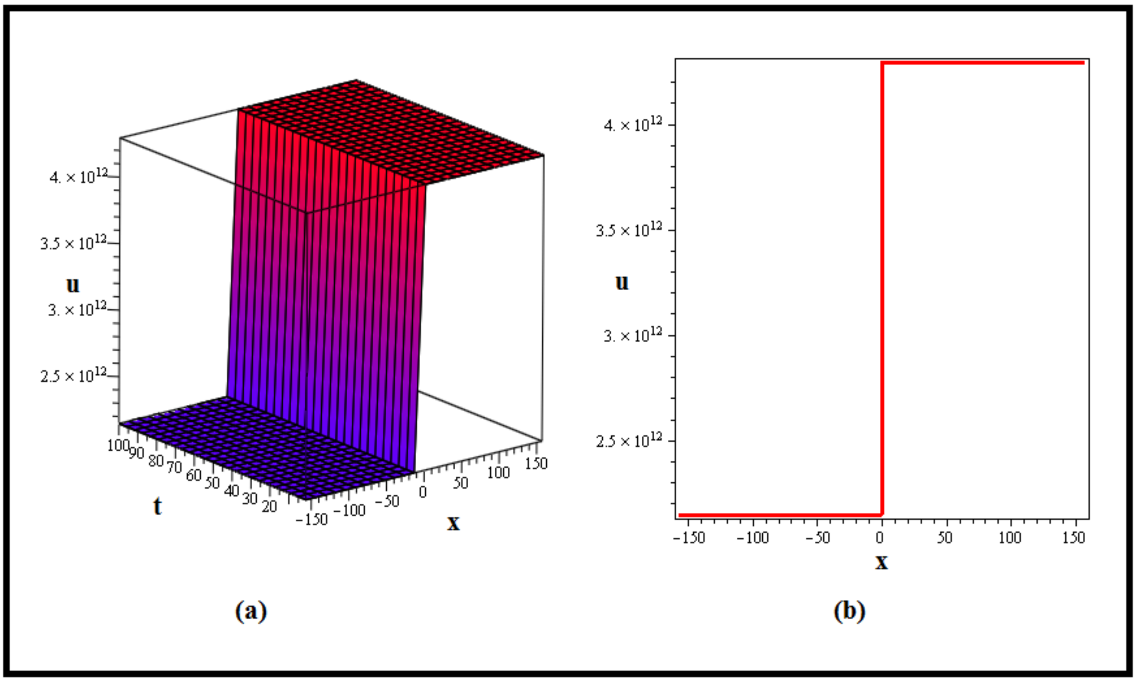

Figure 2. (**a**) The three-dimensional representation of $u_{1,16}$ in Equation (34) is shown with the parameters' values: $a = -50, b = 0, c = 40, \lambda = 100, \kappa = e, r = 10, \beta = 0.9, \rho = 0$. Similarly, (**b**) the two-dimensional graph is constructed using $t = 100$ and the previously specified parameter values. Overall, this profile shows a kink soliton.

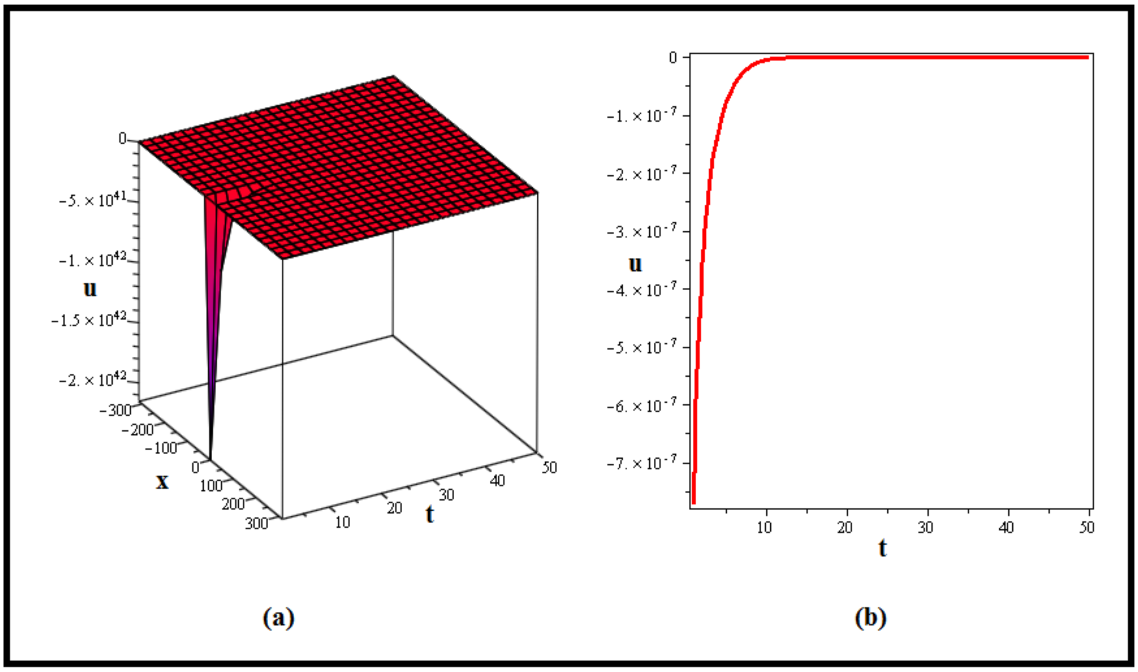

Figure 3. (**a**) The three-dimensional representation of $u_{1,32}$ in Equation (50) is shown with the parameters' values: $a = 0, b = 0, c = 200, \lambda = 50, \kappa = 2, r = 120, \beta = 1, \rho = 1$. Similarly, (**b**) the two-dimensional graph is constructed using $x = -100$ and the previously specified parameter values. Overall, this profile shows a shock soliton.

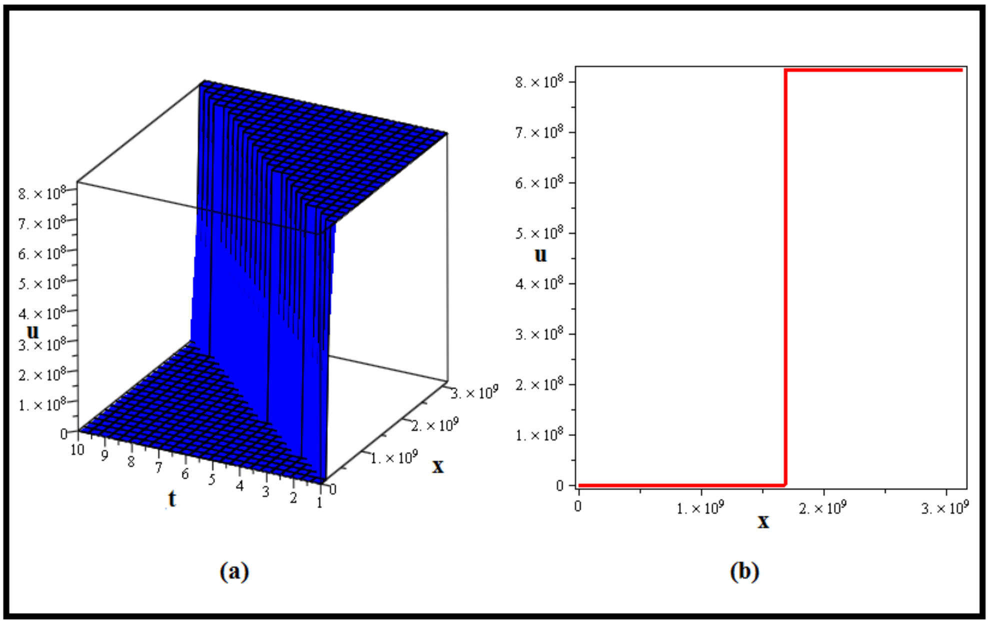

Figure 4. (**a**) The three-dimensional representation of $u_{2,29}$ in Equation (82) is shown with the parameters' values: $a = 70, b = 0, c = -70, \lambda = 100, \kappa = e, r = 200, \beta = 0.9, \rho = 0, q_1 = 100, q_2 = 90$. Similarly, (**b**) the two-dimensional graph is constructed using $t = 6$ and the previously specified parameter values. Overall, this profile shows a periodic kink soliton.

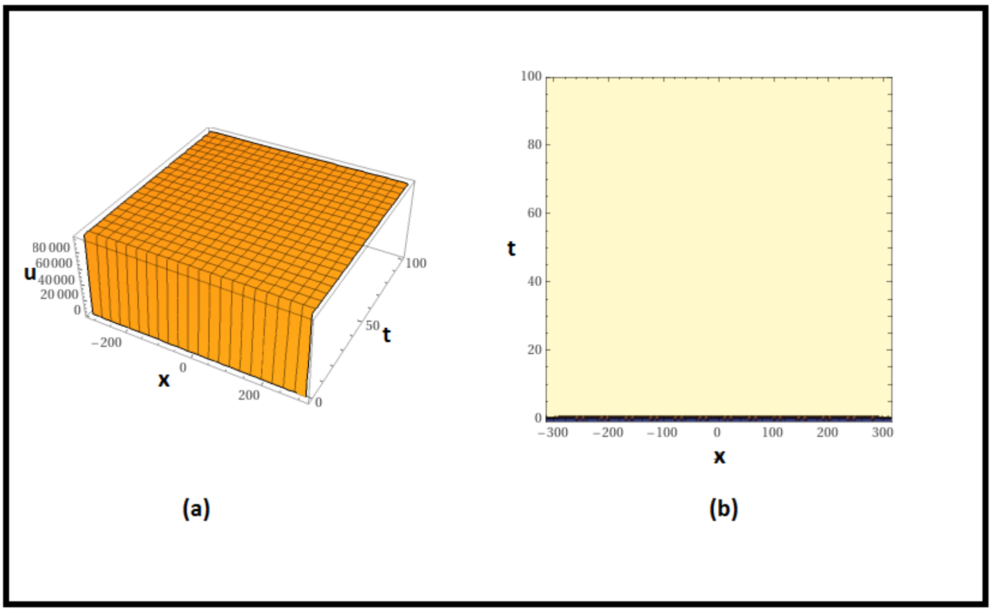

Figure 5. The three-dimensional (**a**) and contour representations (**b**) of $u_{2,16}$ in Equation (69) is shown with the parameters' values: $a = -1, b = 0, c = 5, \lambda = 5, \kappa = e, r = 7, \beta = 0.8, \rho = 0, q_1 = 5$. Overall, this profile shows a singular shock soliton.

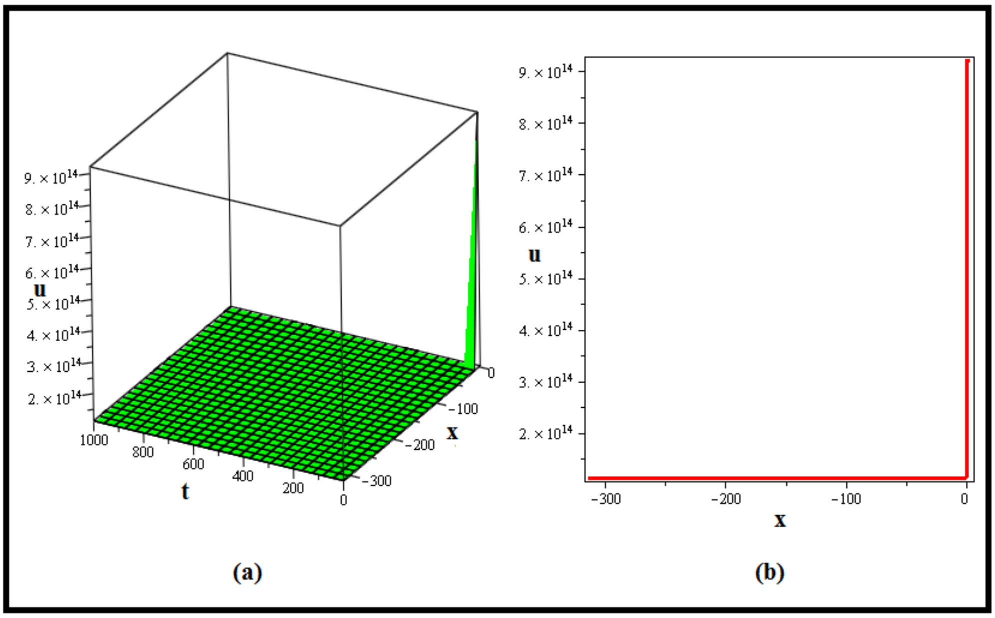

Figure 6. (**a**) The three-dimensional representation of $u_{2,35}$ in Equation (88) is shown with the parameters' values: $a = 0, b = 200, c = 800, \omega = 200, m = 4, \lambda = 160, \kappa = 3, r = 23, \rho = 0, \beta = 1$, $q_1 = 100$, $q_2 = 45$. Similarly, (**b**) the two-dimensional graph is constructed using $t = 0$ and the previously specified parameter values. Overall, this profile shows a singular kink soliton.

6. Conclusions

In conclusion, this work has considerably increased our understanding of the SFKSE by offering a varied variety of singular stochastic soliton solutions in a multiple-noise setting using mEDAM. These answers provide a solid foundation for deciphering complicated physical phenomena regulated by this equation. Using modern computational tools such as the Maple-13 program, we were able to properly visualize the complicated interplay between the stochastic term and SFKSE solutions. While our present analysis has mostly focused on the interaction between multiplicative noise and fractional space, the future of research in this subject seems promising. Future research may focus on additive noise effects and fractional time dynamics, offering a more complete understanding of the SFKSE's multifarious behavior and its larger implications in mathematics, physics, and engineering. Such efforts have the potential to produce useful insights and practical ramifications for real-world circumstances.

Author Contributions: Conceptualization, M.M.A.-S.; Methodology, M.M.A.-S.; Software, H.Y.; Validation, H.Y.; Formal analysis, R.S.; Investigation, R.S. and A.H.G.; Resources, A.H.G. and K.M.; Writing—review & editing, K.M.; Funding H.Y. All authors have read and agreed to the published version of the manuscript.

Funding: This work was supported by the Deanship of Scientific Research, the Vice Presidency for Graduate Studies and Scientific Research, King Faisal University, Saudi Arabia (Grant No. 4454).

Data Availability Statement: Data sharing is not applicable to this article as no new data were created or analyzed in this study.

Acknowledgments: The authors thank the support from the Deanship of Scientific Research, the Vice Presidency for Graduate Studies and Scientific Research, King Faisal University, Saudi Arabia (Grant No. 4454).

Conflicts of Interest: The authors declare no conflict of interest.

References

1. Kamrani, M. Numerical solution of stochastic fractional differential equations. *Numer. Algorithms* **2015**, *68*, 81–93. [CrossRef]
2. Mohammadi, F. Efficient Galerkin solution of stochastic fractional differential equations using second kind Chebyshev wavelets. *Bol. Soc. Parana. Mat.* **2017**, *35*, 195–215. [CrossRef]
3. Abouagwa, M.; Li, J. Approximation properties for solutions to Itô–Doob stochastic fractional differential equations with non-Lipschitz coefficients. *Stoch. Dyn.* **2019**, *19*, 1950029. [CrossRef]
4. Botmart, T.; Agarwal, R.P.; Naeem, M.; Khan, A. On the solution of fractional modified Boussinesq and approximate long wave equations with non-singular kernel operators. *AIMS Math.* **2022**, *7*, 12483–12513. [CrossRef]
5. Mukhtar, S.; Noor, S. The numerical investigation of a fractional-order multi-dimensional Model of Navier-Stokes equation via novel techniques. *Symmetry* **2022**, *14*, 1102. [CrossRef]
6. Alshehry, A.S.; Imran, M.; Weera, W. Fractional View Analysis of Kuramoto-Sivashinsky Equations with Non-Singular Kernel Operators. *Symmetry* **2022**, *14*, 1463. [CrossRef]
7. Alderremy, A.A.; Iqbal, N.; Aly, S.; Nonlaopon, K. Fractional Series Solution Construction for Nonlinear Fractional Reaction-Diffusion Brusselator Model Utilizing Laplace Residual Power Series. *Symmetry* **2022**, *14*, 1944. [CrossRef]
8. Alshehry, A.S.; Yasmin, H.; Ullah, R.; Khan, A. Numerical simulation and analysis of fractional-order Phi-Four equation. *Aims Math.* **2023**, *8*, 27175–27199. [CrossRef]
9. Saha Ray, S.; Das, N. New optical soliton solutions of fractional perturbed nonlinear Schrödinger equation in nanofibers. *Mod. Phys. Lett. B* **2022**, *36*, 2150544. [CrossRef]
10. Mirzazadeh, M. Topological and non-topological soliton solutions to some time-fractional differential equations. *Pramana* **2015**, *85*, 17–29. [CrossRef]
11. Saha Ray, S.; Sagar, B. Numerical soliton solutions of fractional modified (2+1)-dimensional Konopelchenko–Dubrovsky equations in plasma physics. *J. Comput. Nonlinear Dyn.* **2022**, *17*, 011007. [CrossRef]
12. Manafian, J.; Foroutan, M. Application of $\tan(\phi(\xi)/2) tan(\phi(\xi)/2)$-expansion method for the time-fractional Kuramoto–Sivashinsky equation. *Opt. Quantum Electron.* **2017**, *49*, 272. [CrossRef]
13. Zheng, B. Exp-function method for solving fractional partial differential equations. *Sci. World J.* **2013**, *2013*, 465723. [CrossRef]
14. Zheng, B.; Wen, C. Exact solutions for fractional partial differential equations by a new fractional sub-equation method. *Adv. Differ. Equ.* **2013**, *2013*, 199. [CrossRef]
15. Gaber, A.; Ahmad, H. Solitary wave solutions for space-time fractional coupled integrable dispersionless system via generalized kudryashov method. *Facta Univ. Ser. Math. Inform.* **2021**, *35*, 1439–1449. [CrossRef]
16. Khan, H.; Baleanu, D.; Kumam, P.; Al-Zaidy, J.F. Families of travelling waves solutions for fractional-order extended shallow water wave equations, using an innovative analytical method. *IEEE Access* **2019**, *7*, 107523–107532. [CrossRef]
17. Alsharidi, A.K.; Bekir, A. Discovery of New Exact Wave Solutions to the M-Fractional Complex Three Coupled Maccari's System by Sardar Sub-Equation Scheme. *Symmetry* **2023**, *15*, 1567. [CrossRef]
18. Bibi, S.; Mohyud-Din, S.T.; Khan, U.; Ahmed, N. Khater method for nonlinear Sharma Tasso-Olever (STO) equation of fractional order. *Results Phys.* **2017**, *7*, 4440–4450. [CrossRef]
19. Rezazadeh, H.; Mirhosseini-Alizamini, S.M.; Neirameh, A.; Souleymanou, A.; Korkmaz, A.; Bekir, A. Fractional Sine–Gordon equation approach to the coupled higgs system defined in time-fractional form. *Iran. J. Sci. Technol. Trans. A Sci.* **2019**, *43*, 2965–2973. [CrossRef]
20. Yasmin, H.; Aljahdaly, N.H.; Saeed, A.M.; Shah, R. Probing Families of Optical Soliton Solutions in Fractional Perturbed Radhakrishnan–Kundu–Lakshmanan Model with Improved Versions of Extended Direct Algebraic Method. *Fractal Fract.* **2023**, *7*, 512. [CrossRef]
21. Yasmin, H.; Aljahdaly, N.H.; Saeed, A.M.; Shah, R. Investigating Families of Soliton Solutions for the Complex Structured Coupled Fractional Biswas–Arshed Model in Birefringent Fibers Using a Novel Analytical Technique. *Fractal Fract.* **2023**, *7*, 491. [CrossRef]
22. Yasmin, H.; Aljahdaly, N.H.; Saeed, A.M.; Shah, R. Investigating Symmetric Soliton Solutions for the Fractional Coupled Konno–Onno System Using Improved Versions of a Novel Analytical Technique. *Mathematics* **2023**, *11*, 2686. [CrossRef]
23. Mohammed, W.W.; Albalahi, A.M.; Albadrani, S.; Aly, E.S.; Sidaoui, R.; Matouk, A.E. The analytical solutions of the stochastic fractional Kuramoto–Sivashinsky equation by using the Riccati equation method. *Math. Probl. Eng.* **2022**, *2022*, 5083784. [CrossRef]
24. Mohammed, W.W.; Alesemi, M.; Albosaily, S.; Iqbal, N.; El-Morshedy, M. The exact solutions of stochastic fractional-space Kuramoto-Sivashinsky equation by Using (G′ G)-expansion method. *Mathematics* **2021**, *9*, 2712. [CrossRef]
25. Kudryashov, N.A. Solitary and periodic solutions of the generalized Kuramoto-Sivashinsky equation. *arXiv* **2011**, arXiv:1112.5707.
26. Kudryashov, N.A.; Soukharev, M.B. Popular Ansatz methods and Solitary wave solutions of the Kuramoto-Sivashinsky equation. *Regul. Chaotic Dyn.* **2009**, *14*, 407–419. [CrossRef]
27. Wazwaz, A.M. New solitary wave solutions to the Kuramoto-Sivashinsky and the Kawahara equations. *Appl. Math. Comput.* **2006**, *182*, 1642–1650. [CrossRef]
28. Mohammed, W.W. Approximate solution of the Kuramoto-Shivashinsky equation on an unbounded domain. *Chin. Ann. Math. Ser. B* **2018**, *39*, 145–162. [CrossRef]
29. Wazzan, L. A modified tanh–coth method for solving the general Burgers–Fisher and the Kuramoto–Sivashinsky equations. *Commun. Nonlinear Sci. Numer. Simul.* **2009**, *14*, 2642–2652. [CrossRef]

30. Abbasbandy, S. Solitary wave solutions to the Kuramoto–Sivashinsky equation by means of the homotopy analysis method. *Nonlinear Dyn.* **2008**, *52*, 35–40. [CrossRef]
31. Kudryashov, N.A. On types of nonlinear nonintegrable equations with exact solutions. *Phys. Lett. A* **1991**, *155*, 269–275. [CrossRef]
32. Albosaily, S.; Mohammed, W.W.; Rezaiguia, A.; El-Morshedy, M.; Elsayed, E.M. The influence of the noise on the exact solutions of a Kuramoto-Sivashinsky equation. *Open Math.* **2022**, *20*, 108–116. [CrossRef]
33. Bilal, M.; Iqbal, J.; Ali, R.; Awwad, F.A.; A. Ismail, E.A. Exploring Families of Solitary Wave Solutions for the Fractional Coupled Higgs System Using Modified Extended Direct Algebraic Method. *Fractal Fract.* **2023**, *7*, 653. [CrossRef]
34. Liu, P.; Shi, J.; Wang, Z.-A. Pattern formation of the attraction-repulsion Keller-Segel system. *Discret. Contin. Dyn. Syst. B* **2013**, *18*, 2597–2625. [CrossRef]
35. Li, H.; Peng, R.; Wang, Z. On a Diffusive Susceptible-Infected-Susceptible Epidemic Model with Mass Action Mechanism and Birth-Death Effect: Analysis, Simulations, and Comparison with Other Mechanisms. *SIAM J. Appl. Math.* **2018**, *78*, 2129–2153. [CrossRef]
36. Bai, X.; He, Y.; Xu, M. Low-Thrust Reconfiguration Strategy and Optimization for Formation Flying Using Jordan Normal Form. *IEEE Trans. Aerosp. Electron. Syst.* **2021**, *57*, 3279–3295. [CrossRef]
37. Jin, H.; Wang, Z. Boundedness, blowup and critical mass phenomenon in competing chemotaxis. *J. Differ. Equ.* **2016**, *260*, 162–196. [CrossRef]
38. Guo, C.; Hu, J. Fixed-Time Stabilization of High-Order Uncertain Nonlinear Systems: Output Feedback Control Design and Settling Time Analysis. *J. Syst. Sci. Complex.* **2023**, *36*, 1351–1372. [CrossRef]
39. Shi, Y.; Hu, J.; Wu, Y.; Ghosh, B.K. Intermittent output tracking control of heterogeneous multi-agent systems over wide-area clustered communication networks. *Nonlinear Anal. Hybrid Syst.* **2023**, *50*, 101387. [CrossRef]
40. Sarikaya, M.Z.; Budak, H.; Usta, H. On generalized the conformable fractional calculus. *Twms J. Appl. Eng. Math.* **2019**, *9*, 792–799.